# PART I

# INTRODUCTION

# 1

# OVERVIEW OF BIOMEDICAL IMAGE UNDERSTANDING METHODS

Wei Xiong, Jierong Cheng, Ying Gu, Shimiao Li
and Joo-Hwee Lim

*Department of Visual Computing, Institute for Infocomm Research, A*STAR, Singapore*

Computerized image understanding is the process of extracting meaningful features (e.g., color, intensity, and geometry of group of pixels) from the images, inferring and aggregating the symbolic information into unique concepts, matching them with physical world models and producing descriptions of the images and their relationship in the world that the images represent [1]. Biomedical images are those acquired from biology, medicine, pathology, dentistry, and other specialized healthcare domains. With the advancement of modern imaging devices, enormous amounts of digital still and dynamic image data are generated from nano to macro, from protein to cells, and to organs and from animals to human. Computerized image analysis plays an important role in understanding and interpreting these images accurately and efficiently to assist biologists and clinicians in decision making. Being a highly multidisciplinary research field, biomedical image understanding requires knowledge, theories, methods, and techniques from computer science, engineering, mathematics as well as from general and specialized healthcare domains. Developments in related disciplines have rapidly advanced over the past decade. Various imaging modalities and acquiring procedures result in large differences in biomedical images.

---

*Biomedical Image Understanding: Methods and Applications*, First Edition.
Edited by Joo-Hwee Lim, Sim-Heng Ong, and Wei Xiong.

The computerized understanding of these biomedical images requires a few or all of the following essential computational processes:

- Segmentation and object detection
- Registration and matching
- Object tracking
- Classification
- Knowledge-based systems (KBSs).

The schematic diagram in Fig. 1.1 shows the coherent relationships and functions of these basic processes. As a fundamental process in biomedical image understanding, segmentation delineates the image into meaningful regions and unique concepts. These detected regions/objects can be compared with the world models by registration and matching. When analyzing images changing with time, that is, videos, the object motion is tracked and characterized. One way is to first segment the objects and then track them by associating the segmented objects. Some particular features such as shape and context could be extracted for associating. Another way is to perform simultaneous segmentation and tracking.

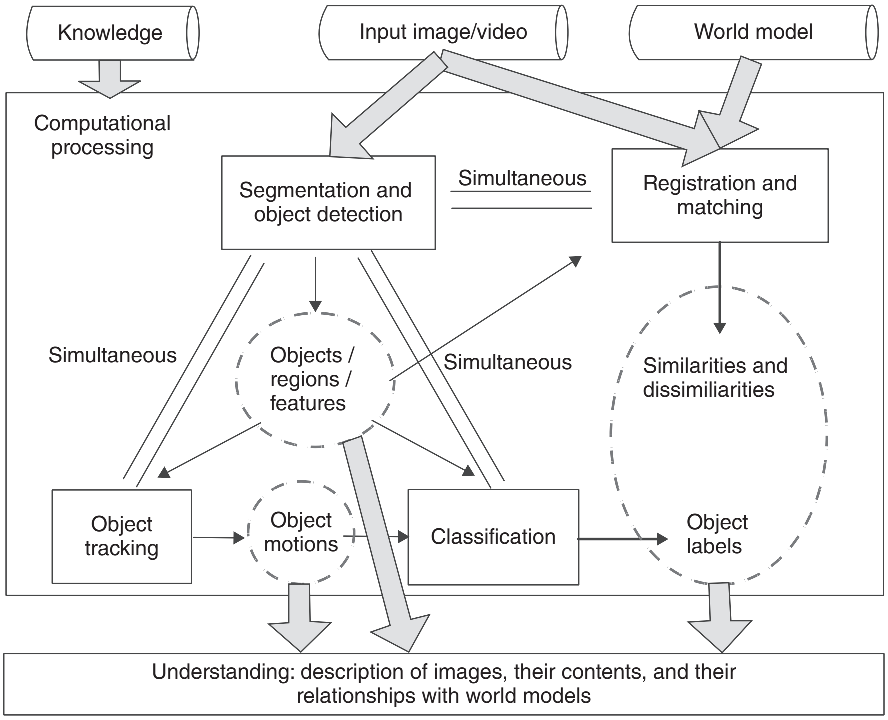

**Figure 1.1** Basic computational processes for image understanding.

Classification is to categorize items into subcategories, such as different attributes, and so on. The output of classification is their labels of different properties. After segmentation, the features, regions, objects, and/or their motions (determined by tracking) may also be further categorized into subclasses. The object motions tracked can also be further classified into different types to enhance the understanding of the deformation and velocity fields in the image. In classifier- or cluster-based segmentation methods, image pixels are grouped into foreground or background and thereby form segments of regions in the image. In such cases, classification and segmentation are processed simultaneously.

Besides segmentation, another fundamental process for the understanding is registration (or matching), which means to align two components for comparisons. Comparing with the world models generates descriptions of similarities and dissimilarities. Registration may not need an explicit clearcut region delineation as input. It may also be used during segmentation, such as atlas construction and multimodal segmentation. Registration may be processed in constituent component levels in images and the detected components come from segmentation or classification.

Segmentation, tracking, and classification involve geometric, structural, and functional features, regions, or objects extracted from the image/video. These features may be from different spaces, represented differently, explicitly, or implicitly.

Whenever necessary and available, knowledge can always be helpful to assist these computation processes. It may be used to initialize a computation, to constrain solution boundaries, to provide feedback on solution feasibility, or as a standard to compare with, and so on. Knowledge could be either prior knowledge or learned during the computation. With prior knowledge, the matching of the above-mentioned symbolic information with world models can be faster, more accurate, more targeted, and/or more robust. Similarity/dissimilarity and labels of objects and their context against the world models in terms of geometry positions, structures, relations, and functions provide primary understanding of the image and its components. Semantic understanding of biomedical images requires the comparisons and matchings with specific domain concepts, models, and knowledge.

In the following sections, we review the above-mentioned essential computational methods and their latest and important applications for the understanding of biomedical images/videos.

## 1.1 SEGMENTATION AND OBJECT DETECTION

Image segmentation is the process of partitioning an image into nonoverlapping, constituent regions that have homogeneous characteristics such as intensity or texture [2]. Let $\Omega$ be the image domain, the segmentation problem is to determine a set of connected subsets $S_i \in \Omega$ that satisfy $\bigcup_{i=1}^{n} S_i = \Omega$ with $S_i \cap S_j = \phi$ when $i \neq j$.

The purposes of segmentation in biomedical images are mainly [3]

- identifying region of interest (ROI);
- measuring organ/tumor volume;

**TABLE 1.1 Taxonomy of Segmentation**

| | | |
|---|---|---|
| Methods based on image processing techniques | | Thresholding [5–7] |
| | | Edge-based methods [8] |
| | | Region-based methods [9–12] |
| Methods using pattern recognition and machine learning algorithms | Supervised classifier methods | *k*-nearest neighbor (KNN) classifier [13, 14] |
| | | Parzen window classifier [15, 16] |
| | | Bayes classifier [17] |
| | Unsupervised classifier methods | *k*-means algorithm [18] |
| | | Fuzzy *c*-mean algorithm [19, 20] |
| | | Expectation-maximization (EM) algorithm [21] |
| Model and atlas-based segmentation | | Parametric active contour models [22] |
| | | Geometric active contour models [23–26] |
| | | Active shape and appearance models [27, 28] |
| | | Atlas-based methods [29, 30] |
| Multispectral segmentation | | Gaussians models with Markov–Gibbs random [31] |
| | | Variational approach for registration [32] |
| | | Feature fusion [33] |
| User interactions in interactive segmentation methods | | Identifying region of interest [34] |
| | | Providing seeds with predefined labels [35, 36] |
| | | Controlling topology [37, 38] |
| | | Correcting segmentation [39, 40] |

*Source*: From Reference [4]

- studying anatomical structure;
- treatment/surgical planning;
- cell counting for drug effect study.

We classify the medical image segmentation methods (Table 1.1) according to Reference [4].

### 1.1.1 Methods Based on Image Processing Techniques

Methods based on image processing techniques have three general categories: thresholding, edge-based methods, and region-based methods. When the ROI or object has homogeneous intensity against a background of different gray levels, one or multiple thresholds can be applied on an image histogram to segment the object from background. Edge-based segmentation relies on the assumption that boundaries between objects are represented by edges, that is, discontinuities in gray level [3]. The discontinuities are usually detected by operators that approximate gradient or Laplacian computation and then used as features in subsequent processes. The performance of various edge-based segmentation approaches was compared in Reference [8].

Region-based segmentation is based on the principal of homogeneity – pixels within each object have similar visual properties [3]. Region growing is a segmentation method that uses a bottom-up strategy. In region growing method [9], a set of seed points are required to initialize the process. Regions are grown iteratively by merging unallocated neighboring pixels depending on a merging criterion. Region growing is usually used in the segmentation of small or simple structures in medical images such as posterior fossa in fetal brain [10], aorta [11], and myocardial wall [12]. Split-and-merge is an algorithm related to region growing, but does not need seed points.

Watershed algorithm [41] is also a region-based segmentation method. It considers the gradient of a grayscale image as a topological relief, where the gray levels represent altitude of the relief. When this relief is flooded from regional minima, the set of barriers built, where adjacent catchment basins meet, is called *watershed*. To handle the problem of potential oversegmentation, region merging and marker-controlled watershed are often used in this type of approaches. Watershed algorithm is the most frequently used method in cell segmentation, especially for clustered nuclei [5–7].

### 1.1.2 Methods Using Pattern Recognition and Machine Learning Algorithms

Due to the artifacts present in medical images, methods solely based on image processing techniques are often used as an initial step in a sequence of image processing operations. More often, these methods are combined with pattern recognition and machine learning algorithms to improve the accuracy of segmentation. Artificial-intelligence (AI) based techniques can be classified into supervised and unsupervised methods. In these methods, the segmentation problem is transformed into a pixel labeling task.

Classifier methods perform supervised segmentation by assigning each pixel to one of the predefined set of classes, which partitions a feature space derived from the image using (training) data with known labels [2]. The *k*-nearest neighbor (KNN) classifier is nonparametric as it does not assume the statistical structure of the data. In KNN method [13, 14], a pixel is classified by a majority vote of its *k*-closest training data. The Parzen window classifier [15, 16] is also nonparametric, in which the classification is made by a weighted decision process within a predefined window of the feature space centered at the pixel of interest. A commonly used parametric classifier is Bayes classifier [17]. It assumes that the pixel intensities are samples from a mixture of Gaussian or other probability distributions. As one of the possible extensions in this paradigm, a fuzzy locally adaptive Bayesian segmentation approach was proposed in Reference [42] for volume determination in positron emission tomography (PET). The Bayesian segmentation model has been applied to segment atherosclerotic plaques [43], skin lesions [44], uterofetal [45], and brain magnetic resonance imaging (MRI) [46].

Clustering methods are unsupervised segmentation methods in which only unlabeled data are used. Commonly used clustering algorithms are *k*-means algorithm [18], fuzzy *c*-means algorithm [19, 20], and the expectation-maximization (EM) algorithm [21]. Traditional clustering algorithms are graph partitioning methods that use a top-down strategy. The partition minimizes the cost function of a constrained optimization problem. Basically, these methods iteratively alternate between segmenting the image (updating labels) and characterizing the properties of each class (updating parameters). The EM algorithm assumes that the data follow a Gaussian mixture model (GMM). The EM algorithm has been used to segment overlapped nuclei in microscopic cell images [47]. Again, many extensions have been attempted, for example, a fuzzy local GMM was proposed in Reference [48] for brain MRI segmentation.

Markov random field (MRF) is a probabilistic model that captures the contextual constraints between neighboring pixels. MRF is often used in a Bayesian framework, and the segmentation is obtained by maximizing *a posteriori* probability, given the image data and prior information. The optimization can be achieved by iterated conditional models or simulated annealing [2]. MRF has been used in segmentation of prostate [49], brain [50–52], spines [53], breast lesion and left ventricle [54], and optic nerve head [55].

### 1.1.3 Model and Atlas-Based Segmentation

AI-based methods can be combined with expert knowledge in the form of rules. When segmenting the organs or structures in medical images, the variation of shape and geometry can be modeled probabilistically. The use of models in medical image segmentation can involve [3]:

1. Registration to training data
2. Probabilistic representation of variations of training data
3. Statistical influence between the model and the target image.

Model-based segmentation methods include deformable models, active shape and appearance model, and level-set-based models [3]. Model-based methods are able to generate closed contours or surfaces directly from images and incorporate a smoothness and/or shape prior constraint on the result contour or surface [2]. However, all the above-mentioned methods need good initialization; otherwise, they are liable to be trapped in local minima. A model-based segmentation algorithm which separates clustered nuclei by constructing a graph on *a priori* information about nucleus properties is proposed in Reference [56].

***1.1.3.1 Parametric Active Contour Models*** The parametric active contour model or snake model was proposed by Kass et al. [22] in 1988. A snake model is parameterized by a sequence of snaxels: $C(s) = (x(s), y(s)), s \in [0, 1]$. This model is sensitive to noise and spurious edges due to the edge terms relying on image gradient information, which may converge to undesirable local minima. The details of snake model and its extensions are given in Section 2.3. One improvement of this model is to include region information, such as the active volume model (AVM) [57]. For some medical images, however, for example, those with complex objects in cluttered backgrounds, the AVM model may fail due to similar appearance between the foreground and some background objects. In these cases, user interactions can help. However, although these interactive methods are convenient, the interaction could be very tedious, for example, users may need to add many attraction points to make the segmentation curve deform to the right edges.

***1.1.3.2 Geometric Active Contour Models*** Geometric active contours are represented implicitly as level sets of a scalar function of high-dimensional variables. The level set approach was first introduced by Osher and Sethian [23] in fluid dynamics. Applying it to image segmentation was simultaneously suggested by Casseles et al. [24] and Malladi and Sethian [25]. Instead of evolving the curve in the plane-like snakes, this geometric functional evolves in time with respect to the *xy* plane. Just as for snakes, we can integrate region information into the level set formulation. A well-known example is the Mumford–Shah functional [26]. The level set method is introduced in Section 2.4.

***1.1.3.3 Active Shape and Appearance Models*** Statistical shape models (SSMs) analyze the variations in shape over the training set to build a model to mimic this variation. The most generic method to represent shapes in SSMs is the use of landmarks: $\mathbf{x} = (x_1, y_1, \dots x_k, y_k)^T$. The usage of prior information makes this approach more robust against noise and artifacts in medical images. The best known SSMs are the active shape model (ASM) [27] and active appearance model (AAM) [28], both by Cootes et al. ASM models the shape using a linear generative model. The optimal model parameters are determined by iteratively searching each point on the shape for a better position and updating the model parameter to best describe the newly found positions. Similarly, AAM jointly models the appearance and shape using a linear generative model. The model parameters are found using a mean square-error criterion and an analysis-by-synthesis approach. A comprehensive review of SSM for 3D medical image segmentation is presented in Reference [58].

***1.1.3.4 Atlas-Based Methods*** Usage of Atlas-based methods is another frequently used approach in medical image segmentation. An atlas is generated by compiling information on the anatomy, shape, size, and features of different organs or structures. The atlas is then used as a reference frame for segmenting new images [2]. Therefore, segmentation can be treated as a registration problem in atlas-based methods. This type of approach is mainly used for magnetic resonance (MR) image segmentation [29, 30]. Multi-atlas construction contains multiple representative atlases from training data and usually works better than single-atlas-based approaches. Multi-atlas segmentation and label fusion have been applied for hippocampal [59] and heart [60] segmentation in MR images and liver segmentation in 3D computed tomography (CT) images [61] recently.

### 1.1.4 Multispectral Segmentation

So far, the image segmentation methods we have discussed were proposed for image data acquired from single modality, for example, MR or CT. Each imaging modality provides distinctive yet complementary information of the structures. In addition, images of the same object can be collected over time in some circumstances.

Segmentation methods based on integration of information from multiple images are called multispectral or multimodal. The use of precise linear combination of Gaussians models to approximate signal distributions and analytical estimates of the Markov−Gibbs random field parameters demonstrated promising results in segmenting multimodal images [31]. A variational approach for multimodal image registration has been introduced in Reference [32], which jointly segments edges via a Mumford–Shah approach and registers image morphologies. Ahmed et al. [33] investigated the efficacy of texture, shape, and intensity feature fusion for posterior-fossa tumor segmentation in multimodal MRI. Surveys on multimodal medical image segmentation methods can be found in References [62] and [63].

### 1.1.5 User Interactions in Interactive Segmentation Methods

Fully automatic, unsupervised segmentation of arbitrary images remains an unsolved problem, especially for medical images. Semisupervised, or interactive segmentation methods with additional human expert knowledge, make the segmentation problem more controlled. However, trade-off must be made between user interaction and performance in any segmentation application. The interactive segmentation methods attempt to minimize the user interactions required and ensure the correctness. Major types of user interaction are listed in the subsequent text according to [64]

- setting parameter values, which is the most common type of interaction;
- selecting seed points for a region growing algorithm;
- drawing initial contour in active contour models;
- selecting constraint points in active contour models [65, 66].

A special type of interaction is user scribbles. The main applications of scribbles are for [64]

- identifying ROI [34] – users can put dots or lines on the objects they want to extract. Good interactive segmentations may potentially arrive at accurate object boundaries;
- providing seeds with predefined labels [35, 36] – users assign labels to some seed pixels. The classification process can take these labeled and unlabeled data points to train a classifier;
- controlling topology [37, 38] – user scribbles are used as a way to control the topologies of segmentations by merging several inhomogeneous regions or splitting homogeneous ones. For instance, users can put a long scribble through the image corresponding to the whole body of a person to indicate that the person's head, neck, torsos, and legs should be connected in the segmentation;
- correcting the result of segmentations [39, 40] – scribbles give users a tool in the correction process of segmentations if needed. Users can make corrections both on labels or on the wrong segmented regions.

It is easy and intuitive to include user scribbles in graph-based segmentations and make the whole process iterative. The graph cut method originally presented by

Boykov et al. [67] uses respective labels to mark the object of interest and its background. The most prominent advantage of the graph-cut-based methods is that they produce a global minimum when there are only two labels involved. Moreover, graph cuts are suitable for interactive interfaces because they minimize the underlying segmentation energy functional directly without the gradual approximating process as in active contour models and thus can return the segmentation results corresponding to the user inputs in a single step. The details of graph cut method can be found in Section 2.5.

### 1.1.6 Frontiers of Biomedical Image Segmentation

Chapter 2 presents three types of segmentation techniques: parametric active contours, geometric active contours, and graph cuts. In the end, a detailed case study of cardiac image segmentation is provided. This case study describes a framework that uses different energy functionals for their respective characteristics, by incorporating a dual-background intensity model, a novel shape prior term, and a weighted method. The experimental results on both CT and MR images show the advantage of the proposed method.

In Chapter 3, segmentation of line-like structure is discussed in the light of retinal vessel segmentation and in the context of retinal image processing (RIA). Three topics are described: vessel width estimation, artery–vein (A/V) classification, and validation. To estimate vessel width from raw binary maps generated by vessel segmentation algorithms, morphological thinning and natural cubic spline fitting are adopted to extract the centerline of vessel segments. Vessel boundaries are then determined by fitting two parallel coupled cubic splines. Previous work on A/V classification is reviewed in Section 3.3.1. Four color features are extracted and classified using a GMM-EM classifier, as described in Section 3.3.2. Finally, important issues in validation of RIA software are presented.

Chapter 4 focuses on segmentation of small objects, namely, cell nuclei. For completeness, the chapter covers the following aspects using a case study: (1) a general region-based geometric feature developed for detection of mutants in skin cell images, which works for image patches with random size and shape, (2) spot and clustering detection based on image processing techniques, (3) a Mumford–Shah model with ellipse shape constraint for cell nucleus segmentation, overcoming the limitations of edge-based method and without the need of initial conditions, (4) a mitotic cell classification method with the novel exclusive independent component analysis (XICA), and (5) endometrial image segmentation using texture features and subspace Mumford–Shah segmentation model.

## 1.2 REGISTRATION

Image registration, along with segmentation, has been one of the main challenges in image analysis and understanding. Registration involves two images defined in the image domain $\Omega$ – the moving (or source) image $M$ and the fixed (or target) image $F$ – related by a transformation $\mathbf{T}$ parametrized by $\theta$ and operated on $M$. The goal of registration is to estimate the optimal transformation that optimizes an energy function

$$\mathcal{S}(F, \mathbf{T}_{\boldsymbol{\theta}} \circ M) + \alpha \mathcal{R}(\mathbf{T}_{\theta}), \tag{1.1}$$

where $\mathcal{S}(.,.)$ is a similarity measure quantifying the quality of the alignment, $\mathcal{R}$ regularizes the transformation to favor any specific property in the solution or to tackle the difficulty associated with the ill-posedness of the problem [68], and $\alpha$ is a coefficient balancing the two terms.

The transformation $\mathbf{T}$ is a mapping function of the domain $\Omega$ to itself, which maps point locations to other locations. The transformation $\mathbf{T}$ at every position $\mathbf{x}$ can be written as a vector field form with displacement or deformation $\mathbf{u}$:

$$\mathbf{T}_{\boldsymbol{\theta}}(\mathbf{x}) = \mathbf{x} + \mathbf{u}(\mathbf{x}). \tag{1.2}$$

Registration facilitates the interpretation of associated biomedical images by establishing correspondence among multiple sets of data from their structure, anatomy, and functionality and their surrounding regions. Registration can be applied to (1) fusion of multimodality imaging data to provide image-guided diagnosis, treatment planning, or surgery; (2) study of structural or anatomical changes over time; and (3) modeling of population and construction of statistical atlases to identify variation [68].

A well-cited survey of general registration techniques in the early 1990s was presented by Brown in Reference [69] and those applicable to medical images were reviewed in Reference [70] by Calvin in 1993. Two widespread and systematic reviews on medical image registration are done in References [71] and [72]. Zitova and Flusser [73] added comprehensive review for newly developed techniques in 2003. A review of cardiac image registration methods was presented by Makela et al. [74] in 2002. Most recently, elastic medical image registration has been reviewed in Reference [75] (2013), shape-based techniques are introduced in Reference [76] (2013), and medical image registration techniques are revisited in Reference [77] (2013).

### 1.2.1 Taxonomy of Registration Methods

There exists a variety of customized techniques developed in the past 30 years and they can be classified in terms of the imaging modality, dimensionality of $M$ and $F$, type of features for registration, models of transformation $\mathbf{T}$, user interaction, optimization procedure, subject of the registration, and objects (the part of the anatomy). Furthermore, the techniques also differ in the design of similarity measures $\mathcal{S}$ for the matching of $M$ and $F$.

***1.2.1.1 Dimensionality*** The dimensionality of $M$ and $F$ may be of two or three and hence registration can be transformed from 2D to 2D, from 3D to 3D, from 2D to 3D, or from 3D to 2D spaces. 2D/2D registration is usually faster than 3D/3D registration as fewer points are involved. 2D/2D registration is to align planar image objects. It may be applied to locate, align, and compare different scans or X-ray images, and so on [78]. 3D/3D registration establishes correspondences of points in two volumes. For example, fusion of 3D MR/PET and CT volumes involves 3D/3D registration. Morphological tools were explored to register 3D multimodality medical images [79] to extract similar structures from the images and enable rigid registration by simple morphological operations.

3D/2D registration is an ill-posed problem as it is to find correspondence of points in a plane (a projection of a 3D volume or a slice section of a volume) to their counterparts in another volume. It is widely applied in computer-assisted image-guided intervention [80, 81], where $M$ is the preintervention anatomy model and $F$ is the personalized or intraintervention images of the respective anatomy [82].

#### 1.2.1.2 Features for Registration

The features used for registration can be extrinsic (from outside the data sets) or intrinsic (within the data sets). Extrinsic registration uses fiducial or markers [83] or stereo tactic frames [84]. They are normally fast using rigid transforms. However, the features may be decoupled with the data sets, thereby introducing decoupling correspondence errors. Intrinsic registration techniques use features derived within the data sets, such as landmarks, segmented geometrical objects (boundaries, edges, etc.) [85], voxel intensities [71], and so on. In the latter class of registration techniques, features may be difficult to extract. However, as they are derived from the images, the decoupling error is removed.

#### 1.2.1.3 Transformation Models

The model of the transformation **T** can be rigid, affine, projective, nonrigid (deformable, elastic), and so on. Registration techniques based on these models are summarized in Table 1.2.

*Rigid and Affine Transformation.* In the case of rigid objects, only translation and rotation are considered. This type of transformations can provide a global alignment of the data sets quickly as fewer parameters are involved. It is normally used for coarse registration [86]. A well-known and efficient method is the interactive closest point algorithm [87]. Affine transformation, which allows for scaling and shearing, involves more parameters to be decided in the registration. In many situations, affine transformation would be sufficient for the alignment of objects [88]. Note that, for rigid registrations, the transformation **T** is not a function of the position **x**.

**TABLE 1.2 Taxonomy of Transformation Models for Registration**

| | |
|---|---|
| Rigid and affine transformation | Coarse registration [86]<br>Interactive closet point algorithm [87]<br>Affine transformation [88] |
| Nonrigid transformation | Spline-based registration [89–92]<br>Elastic model [93–96]<br>Fluid registration [97–100]<br>Diffeomorphic registration [97, 98, 101–104] |

*Source*: From Reference [77]

*Nonrigid Transformation.* A large portion of biomedical image registration techniques utilize nonrigid transformations. Nonrigid registration or deformable registration is used interchangeably in the literature. In nonrigid registrations, the transformation **T** is a function of the position **x**. Holden [105] presented a comprehensive review of the geometric transformations for nonrigid body registration. General nonrigid registration theory and applications were surveyed in Reference [106] (in 2004) and later expanded by Sotiras in Reference [68] for deformable registrations in 2012.

*Spline-Based Registration.* Note that $M$ and $F$ are given as digital images that are discrete. Using their image pixels as control points, continuous curves, surfaces, and volumes can be constructed using approximation, interpolations, or extrapolations with various kernels such as splines. The continuous forms of data allow direct derivative computation during registration optimization. Moreover, spline-based registration utilizes information apart from the original data points; hence, it is expected to achieve more accurate correspondence. The famous thin plate spline (TPS) technique [89] was widely used in many applications such as biological sample shape comparisons [90–92]. TPS can generate sufficient smooth surfaces as all available data are employed as control points. However, the influence of the data points that are far away from the current computation point is included in the approximation. Hence, the TPS is not spatially well “localized.”

B-spline is defined using a few vicinity control points. Errors in determining the position of one control point only affect the transformation in the neighborhood of that point. Hence, B-spline-based techniques have better locality. B-splines have been widely applied in the registration of images of the brain [107], the chest [108], the heart [109], and so on. However, as there are only a few control points in B-spline approximation, there is a danger of causing folding of the deformation field. Therefore, some measures need to be taken, for example, to enforce intensity consistency in the underlying local image structure or to include a bending energy in the constraints [110]. Sorzano et al. [111] proposed a vector spline regularization, which provides some control over two independent quantities that are intrinsic to the deformation: its divergence and its curl. This is useful when parts of the images contain very little information or when its repartition is uneven.

*Elastic Models.* Elastic registration, introduced by Broit [93] in 1981, expects the deformation field **u**, with a “force” of constrain **f**, to follow certain elastic equation:

$$\mu\nabla^2\mathbf{u} + (\beta + \mu)\nabla(\nabla \cdot \mathbf{u}) + \mathbf{f} = 0, \tag{1.3}$$

where $\mu$ and $\beta$ are coefficients describing rigidity and elasticity in solid mechanics. The problem is to design **f** to lead to correct registration. Hence, **f** is often derived from the images, for example, from the contours [94]. Elastic modeling [95] cannot handle large deformations, that is, it can only handle small displacement **u**. One way to handle this challenge is to initialize the two images close enough or use multiple resolutions to align the images in a few passes [94]. HAMMER [96] forms the elastic registration as another optimization problem. It utilizes a hierarchical attribute matching mechanism to reflect the underlying anatomy at different scales. Applied to register magnetic resonance images of the brain, it demonstrates very high accuracy.

*Fluid Registration and Demons Algorithm.* Elastic modeling is based on linear elasticity assumption that the deformation energy caused by stress increases proportionally with the strength of the deformation. Therefore, it has limits in modeling local nonlinear deformations. Fluid registration [97] relaxes the constraints of elastic modeling by introducing a time dimension $t$. This enables the modeling of highly localized deformations including corners. Such a property is very useful for intersubject registration (including atlas matching), where there are large deformations and/or large degrees of variability and localized deformations. Let $\mathbf{v}$ be the velocity of $\mathbf{u}$ over time $t$, and $\mathbf{b}$ be a distributed body force. The fluid registration expects the deformation that follows the fluid equation:

$$\mu\nabla^2\mathbf{v} + (\beta + \mu)\nabla(\nabla \cdot \mathbf{v}) + \mathbf{b}(\mathbf{u}) = 0. \tag{1.4}$$

The registration problem is to specify an appropriate $\mathbf{b}$ for the registration. Computation of the fluid registration is expensive. Morten and Claus proposed a much faster approach utilizing the linearity of the deformation of the velocity field of the fluid in a scale-space framework [98]. Thirion [99] proposed the famous “Demons” algorithm that considers the registration and matching as a diffusion processing. It is an approximation to the fluid registration. For a survey of nonlinear registration methods, the reader is refereed to [100].

*Diffeomorphic Registration.* In mathematics, a diffeomorphism is an isomorphism in the category of smooth manifolds. It is an invertible function that maps one differentiable manifold to another such that both the function and its inverse are smooth. Diffeomorphisms preserve the topology of the objects and prevent folding. Early diffeomorphic registration approaches were based on the viscous fluid field [97] using finite difference methods to solve Eq. (1.4). Diffeomorphic registration can account for large displacements preserving the warped image without tearing or folding. Viscous fluid methods have to solve large sets of partial differential equations. The earliest implementations were computationally expensive as the inefficient successive overrelaxation approach is used [97]. Later, Fourier transforms are utilized to improve the computation [98]. More recent algorithms attempt to find quickly solvable subproblems by updating parameters iteratively [101–103]. Now the diffeomorphic-demons algorithm proposed by Vercauteren is widely used [104] and the improvements are still ongoing.

### 1.2.2 Frontiers of Registration for Biomedical Image Understanding

Normalized mutual information (NMI) as similarity to measure the goodness of registration is frequently used as it does not need explicit correspondence. Currently, only a discrete joint histogram is considered for the computation of NMI. As a result, explicit derivative of the cost function is not available. Therefore, only nonparametric techniques, such as hill climbing, instead of gradient-based approaches, can be used to optimize the registration.

Chapter 5 presents a nonrigid registration method using continuously represented NMI. The authors propose a method to estimate the Parzen windows, which are used to analytically represent parametrized marginal and joint histograms and hence the NMI and its derivative. They also provide theoretical analysis and experimental comparisons of the performance of the designed kernel and the B-spline. The proposed registration method is applied to magnetic resonance image-guided efficient interventional therapy of liver tumors using microwave thermocoagulation. As closed-formed derivatives can be derived, the histograms and hence the NMI can be readily computed, gradient-based optimization methods can be used and this results in 50% less computation costs and hence much faster registration.

Abdominal aortic aneurysm (AAA) is a localized ballooning of the abdominal aorta. During endovascular aneurysm repair (EVAR)of AAA, real-time intraoperative 2D X-ray imaging is needed by fusing the images with high-resolution preoperative CT 3D data to provide realistic artery anatomy during the navigation and deployment of stent grafts [112]. The real-time and accurate requirements impose challenges in the 2D/3D registration methods.

To tackle these challenges, Chapter 6 first employs a rigid transformation with complementary information provided by one contrast-filled abdominal aorta image and one noncontrast spine image to achieve accurate 2D/3D registration in 3D space globally with decoupled parameter space based on the prior knowledge of the image acquisition protocol during EVAR and a hierarchical registration scheme. Next, a deformable transformation is used to cope with local deformable movements during EVAR. A 3D graph is generated to represent the vascular structure in 3D, and a 2D distance map is computed to smoothly encode the centerline of the vessel. The deformable registration based on 3D graph needs only a few seconds and is very accurate in submillimeter errors using only one single contrast-filled X-ray image. Finally, to cope with patient movements during EVAR, pelvis upper boundary is automatically detected and overlaid onto the fluoroscopic image during the stenting procedure to observe patient movement real-time and to trigger automatic 2D/3D re-registration of the abdominal aorta.

## 1.3 OBJECT TRACKING

Object tracking is an important technique involved in many computer vision applications. The object tracking algorithms have been widely used in computers, video cameras, and automated video analysis. Object tracking is defined as the process of segmenting an object of interest from a video scene and keeping track of its motion, orientation, and occlusion, and so on, so as to extract useful information. The first relevant step of information extraction is the detection of the moving objects in video scene. The next steps are the tracking of such detected objects from frame to frame and the analysis of the object tracks to analyze their behavior. Significant progress has been made in motion tracking during the past few years. Many object tracking

**TABLE 1.3 Taxonomy of Tracking**

| | | |
|---|---|---|
| Object representation | | Points [118, 119]<br>Primitive geometric shapes [120]<br>Object silhouette and contour [121]<br>Articulated shape models [122]<br>Skeletal models [123, 124] |
| Feature selection for tracking | Manual feature selection | Color [125]<br>Edges [126]<br>Optical flow [127–131]<br>Texture [132–135] |
| | Automatic feature selection | Filter methods [136, 137]<br>Wrapper methods [138–140]<br>Embedded methods [15, 141, 142] |
| Object tracking technique | | Point tracking [118, 143–146]<br>Kernel tracking [120, 147–150]<br>Silhouette tracking [151–156] |

*Source*: From References [113, 114]

methods have been developed (see, e.g., [113–117]). They differ from each other based on the way they approach in the following aspects:

- Which object representation is appropriate?
- Which image features should be used?
- How should the motion, appearance, and shape of the object be modeled?

Numerous tracking methods have been proposed for a variety of scenarios. We will provide comprehensive review (Table 1.3) from the three aspects mentioned earlier according to [113, 114].

### 1.3.1 Object Representation

The first issue is defining a suitable representation of the object. Objects can be represented by their shape and appearances. The representation commonly employed for tracking is given as follows:

(1) *Points*. The object is represented by points [118, 119]. This representation is suitable for tracking objects that have small regions in an image.

(2) *Primitive Geometric Shapes*. Object shape is represented by a rectangle or ellipse [120]. Such representation is used to model object motion by translation, affine, or projective transformation.

(3) *Object Silhouette and Contour*. Contour representation defines the boundary of an object. The silhouette of an object means the region inside the contour. Silhouette and contour representations are suitable for tracking complex nonrigid shapes [121].

(4) *Articulated Shape Models*. Articulated objects are constructed of joint body parts [122].

(5) *Skeletal Models*. The skeletal models are commonly used as a shape representation for recognizing objects [123, 124], and such a representation can be used to model both articulated and rigid objects.

There are different ways to represent the appearance features of objects. The shape representations and appearance representations can be combined together for tracking. Some general appearance representations for object tracking are probability densities of object appearance [120, 157–159], templates [160], AAMs [161], and multiview appearance models [149, 162].

### 1.3.2 Feature Selection for Tracking

The most attractive property of a feature is its uniqueness so that the objects can be easily distinguished in the feature space. The objectives of feature selection are multifold. The details of common visual features are as follows according to [113]:

1. *Color*. The apparent color of an object is affected primarily by two factors, namely, the spectral power distribution of the illuminant and the surface reflectance properties of the object [125]. Among all the features, color is one of the most widely used. However, these color spaces are sensitive to noise.
2. *Edges*. Object boundaries usually change along with image intensities. Edge detection is used to identify these changes. Notice that edges features are less sensitive to illumination changes compared to color features. An evaluation of the edge detection algorithms is provided by Reference [126].
3. *Optical Flow*. Optical flow is commonly used as a feature in motion-based segmentation and tracking applications. Popular techniques for computing optical flow include those given in References [127–131].
4. *Texture*. Texture is to measure the change of intensity of a surface with smoothness and regularity. Compared to color, texture requires a processing step to generate the descriptors, such as gray-level cooccurrence matrices (GLCMs) [132], Law’s texture measures [133], wavelets [134] , and steerable pyramids [135]. The texture features are less sensitive to illumination changes compared to color as edge features.

Features are mainly chosen manually contingent on the application domain. Now, users pay large attention to the problem of automatic feature selection, which can be divided into [113, 114]:

- *Filter Methods* [136, 137]. The filter methods select the features based on a general criteria, and find a good feature subset independently of the model selection step. The advantages are that they are easily scaled to very high-dimensional datasets, computationally simple and fast, and are independent of the classification algorithm. But they ignore the interaction within the classifier.

- *Wrapper Methods* [138–140]. The wrapper methods put the model hypothesis search within the feature subset search. The advantages include the interaction between feature subset search and model selection, and the ability to take into account feature dependencies. A common drawback is that they are more likely over fitting than filter techniques and are very computationally intensive.
- *Embedded Methods* [15, 141, 142]. The embedded methods can be considered as a search in the combined space of feature subsets and model hypothesis. The advantage is the interaction with the classification model, meanwhile being far less computationally intensive than wrapper methods.

### 1.3.3 Object Tracking Technique

The goal of object tracking is to generate the trajectory of an object over time by locating its position in every frame of the scene. The tasks of detecting the object and setting up correspondence across frames can either be performed separately or jointly. When performed separately, the object regions in every frame are obtained through object detection algorithm, and then the tracker corresponds to objects across frames. When performed jointly, the object region and correspondence are jointly estimated by iteratively updating object location and region information obtained from previous frames. We now briefly introduce the main tracking categories [113]:

1. *Point Tracking*. Tracking can be elaborated as the correspondence of detected objects represented by points across frames. Indeed, point tracking methods can be divided into deterministic [118, 143] and statistical methods [144–146]. The deterministic methods use qualitative motion [118] to constrain the problem, while probabilistic methods consider the object measurement and uncertainties to establish correspondence.
2. *Kernel Tracking*. Kernel tracking is performed by computing the motion of the object, represented by a primitive object region across the frame. The object motion is usually in the form of parametric motion or the dense flow field computed in subsequent frames. We divide the kernel tracking methods into two categories: templates and density-based appearance models [120, 147, 148], and multiview appearance models [149, 150].
3. *Silhouette Tracking*. Objects may have complex shapes that cannot be well described by simple geometric shapes. Silhouette-based methods can provide a more precise shape description for such objects. We divide silhouette tracking methods into two categories: shape matching [151–153] and contour tracking [154–156].

### 1.3.4 Frontiers of Object Tracking

Chapter 7 presents a detailed description of three tracking techniques: point tracking, silhouette tracking, and kernel tracking, each with a well-known representative method, namely, Bayesian tracking methods (Section 7.3), deformable tracking models (Section 7.4), and harmonic phase algorithm (Section 7.5). A detailed case study of cardiac motion tracking in myocardial perfusion MRI is also included in this chapter. It presents a nonrigid registration method using spatiotemporal smoothness constraint and seeking the global optimal deformation for the entire sequence by introducing the pseudo ground truth (PGT).

## 1.4 CLASSIFICATION

A pattern can be treated as a vaguely defined entity that could be given a name contrary to a chaos [163]. The primary goal and approach in pattern classification is to process the sensed raw data and choose the best-fitted model for any sensed pattern [15]. With the development of research on KBSs, pattern classification has progressed to a great extent and been successfully applied in various scientific and engineering problems such as biometric recognition, medical diagnosis, computer vision, and remote sensing. Machine learning approaches and methods imported from statistical learning theory have been most intensively studied and used in this subject.

The aim of pattern classification is to assign a given pattern to one of the $c$ categories $\omega_1, \omega_2, ..., \omega_c$ based on a vector of $d$ feature values $\mathbf{x} = (x_1, x_2, ..., x_d)$. A pattern classification system involves a number of essential processes: data acquisition and preprocessing, segmentation, feature extraction, classification/decision making, to name a few (Fig. 1.2). *Models* are descriptions of patterns in mathematical form [15]. At the beginning of designing a pattern classification system, hypothesis of the class of models has to be formulated. *Preprocessing* is used to reduce data complexity and/or variation and it is typically applied before feature extraction to permit/simplify feature computations. Sometimes *segmentation* is needed to separate the objects of interest in the images from the background. The purpose of *feature extraction* is to reduce the data complexity and uncertainty further by measuring only certain features or properties of the (image of) objects to be classified [15]. A *classifier* takes the features as input and makes the final decision on which class of the models the input should belong to. We can use *training samples* to build the classifier and *testing samples* (unseen data) to test its performance. We need to define the *cost* or consequences of the action (i.e., classification and decision).

The central task in pattern classification is to construct or learn a decision rule so as to minimize the cost [15]. More specifically, we aim to find an optimal decision boundary to separate different classes in the feature space. However, a good classifier is not designed to separate all training samples perfectly, but to suggest correct decisions when presented with novel patterns. An overly complex model is likely to cause *overfitting*, as opposed to *generalization*. A trade-off has to be made between the performance on training samples and the simplicity of the classifier. It is generally accepted that using at least 10 times as many training samples per class $n$ as the number of features $d$ (n/d>10) is a good practice to follow in classifier design [165]. The more complex the classifier, the larger should the ratio of sample size to dimensionality be to avoid the curse of dimensionality.

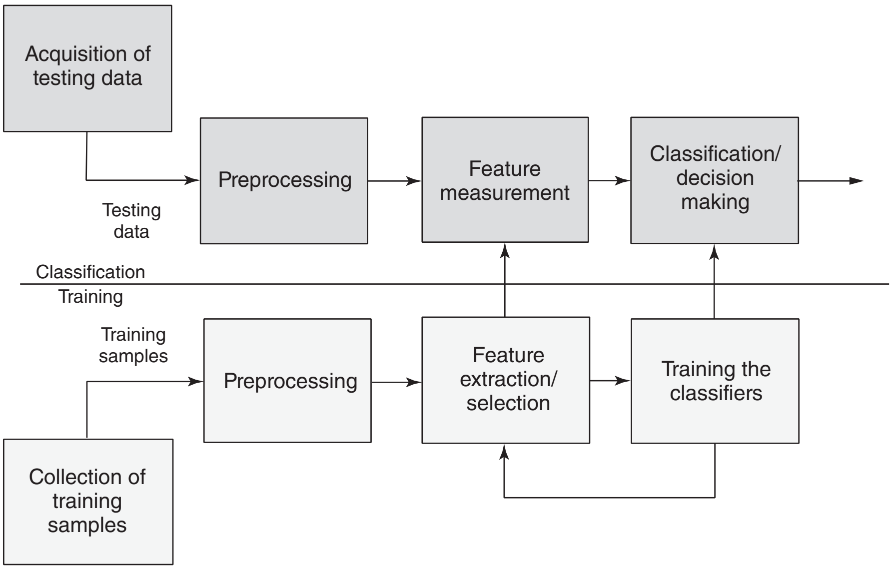

**Figure 1.2** Model of pattern classification system [164].

In the subsequent subsections, we go through some important issues in pattern classification in more detail.

### 1.4.1 Feature Extraction and Feature Selection

Feature extraction methods are used to determine an appropriate subspace of dimensionality $m$ in the original feature space of dimensionality $d$ ($m < d$) [164]. The function that maps the original input data into the new feature space can be linear or nonlinear. The best known linear feature extractor is principal component analysis (PCA) or Karhunen–Loéve transform. PCA identifies the eigenvectors with the largest eigenvalues to represent (Gaussian) data according to a minimum-square-error criterion [164]. Nonlinear PCA can be achieved using a five-layer neural network with an autoassociator or autoencoder technique – each pattern is presented as an input and as an target output. Independent component analysis (ICA) [166, 167] is a method to find a linear representation of non-Gaussian data so that the components are statistically independent. It is an unsupervised method that can be applied to the problem of blind source separation. Discriminant analysis is a supervised method in which interclass separation is emphasized [168].

Kernel PCA [169] performs nonlinear feature extraction by mapping data into a new feature space via some integral operator kernel functions. Another example of nonlinear feature extraction method is multidimensional scaling (MDS) [170]. The MDS method represents multidimensional data points as points in lower dimensional space whose interpoint distances correspond to similarities or dissimilarities.

Given a set of features $Y$, feature selection is sometimes required to select a subset $X \subseteq Y$ that leads to the smallest classification error from the extracted features. Sequential forward selection (SFS) [171, 172] starts with the best single feature and adds one feature at a time so that selected features maximize a criterion function. Reversely, sequential backward selection (SBS) [171, 172] starts with all the features and deletes one feature at a time. "Plus $l$-take away $r$" and sequential floating search methods repeat forward and backward selection alternatively to give better performance. The correlation feature selection (CFS) measure [173] gives high scores to subsets that include features highly correlated to the classification but have low correlation to each other. Peng et al. [174] proposed a minimum-redundancy-maximum-relevance (mRMR) feature selection method that can use mutual information, correlation, or distance/similarity scores to select features. Auffarth et al. [175] compared different redundancy and relevance measures for feature selection in tissue classification in CT images. In their paper, a "value different metric" (VDM) was proposed, which is very good as both redundancy and relevance measurement. The mRMR and SFS algorithms are also reviewed in Section 10.2.3.

One fundamental issue in feature selection (as well as in classification and clustering) is how to measure the similarity or dissimilarity between samples. Metric learning concerns with learning effective distance metrics in feature space. An overview of metric learning algorithms including PCA is also presented in Section 10.2.3.

### 1.4.2 Classifiers

Three types of approaches to classifier design have been identified [164] (Table 1.4). The first approach is simple and intuitive: patterns are assigned to the most similar template. In template matching method [176], patterns are classified based on a metric that is established to define similarity and a few prototypes in each class. In nearest mean classifier [168], each class is represented by the mean vector of all training patterns in that class. One-nearest neighbor (1-NN) classifier [177, 178] gives robust performance in most applications and no training is needed.

The second approach is based on the optimal Bayes decision rule, which assigns a pattern to the class with the maximum posterior probability [179]. The Bayes decision rule combines the likelihoods and the prior probabilities to achieve the minimum probability of error [164]. The Bayes decision rule coincides with maximum likelihood decision rule when the prior probabilities are equal and a 0/1 loss function is used. This rule yields linear or quadratic decision boundary for Gaussian distributions. In Section 8.2.2, the Bayesian decision theory is briefly reviewed. In real-life problems, the true prior probabilities and the class conditional probability density function (pdf) are unknown. In *generative* models, the estimates of priors and pdfs are used in place of the true densities. Some density estimates are parametric, such as linear discriminant classifier (LDC) and quadratic discriminant classifier (QDC) [180]. The others are nonparmateric, for example, $k$-nearest neighbor (KNN) rule and the Parzen classifier [15]. A description of KNN algorithm can be found in Section 10.2.2.

**TABLE 1.4 Taxonomy of Classifiers**

| | | |
|---|---|---|
| Intuitive approach (based on concept of similarity) | | Template matching [176]<br>Nearest mean classifier [168]<br>1-nearest neighbor rule [177, 178]<br>*k*-nearest neighbor classifier [15]<br>… |
| Probabilistic approach (based on Bayes decision rule) [179] | Parametric methods | Linear discriminant classifier [180]<br>Quadratic discriminant classifier [180]<br>… |
| | Nonparametric methods | Parzen windows classifier [15]<br>… |
| Geometric approach (to construct decision boundaries) | Linear methods | Linear support vector machine (SVM) [185]<br>Single-layer perceptron neural network [181]<br>… |
| | Nonlinear methods | Kernel-SVM [186]<br>Multilayer perceptron neural network [172]<br>Radial basis network [172]<br>Decision tree [182, 184]<br>… |

*Source*: From Reference [164]

The third approach is to construct decision boundaries by minimizing certain error criterion. For example, Fisher's linear discriminant minimizes the mean squared error (MSE) [180] and the single-layer perceptron [181] updates the separating hyperplane based on the distances between the misclassified patterns and the hyperplane. Structural approximations of the discriminant functions include tree classifiers [182], multilayer perceptrons (MLPs) [172], radial basis functions (RBFs) [172], and combination of classifiers such as Adaboost [183]. MLP iteratively optimizes MSE of two or more layers of perceptrons using sigmoid transfer function. The hidden layers in MLP allow nonlinear decision boundaries. RBF iteratively optimizes MSE of a feedforward neural networks using Gaussian-like transfer functions. Decision trees [182, 184] are trained by iteratively selecting individual features at each node of the tree. In the more recently developed support vector machine (SVM) [185], the margin between the classes is maximized by selecting a minimum number of support vectors – the training patterns nearest to the decision boundary. The formulations in SVM can be found in Section 8.2.4. In contrast with generative models, the classifier design methods that approximate the decision boundaries or discriminant functions empirically are referred as *discriminative* models.

### 1.4.3 Unsupervised Classification

So far, we have discussed supervised classification in which an input pattern is identified as a member of a predefined class. Next, we move on to a very different problem: unsupervised classification or clustering, in which the pattern is assigned to an unknown class. The key questions in clustering are [187]:

- Is there a structure in the data?
- How many clusters are there in the data?
- How do we select an appropriate measure of similarity to define cluster?
- How do we evaluate the clustering results?

Two popular clustering techniques are iterative square-error partitional clustering and agglomerative hierarchical clustering [164]. Hierarchical techniques merge similar clusters at each iteration, for example, single linkage clustering and complete linkage clustering [187]. Partitional clustering techniques assign all points to a cluster in each iteration, such that the within-cluster scatter is minimized or the between-cluster scatter is maximized. A typical example is $k$-means algorithm [188] to which the number of clusters $k$ and the initial cluster centers have to be given. Fuzzy $c$-means [20] clustering is very similar to $k$-means algorithm except that each pattern has a degree of membership to all clusters rather than assigned to only one cluster. In the mean shift algorithm [189], a window of kernel function is moved by a mean shift vector iteratively. The mean shift vector always points toward the direction of the maximum increase in the density.

Another popular partitional clustering technique is mixture decomposition. In this algorithm, each pattern is assumed to be drawn from of $k$ underlying clusters [164]. Cluster parameters and the number of components are estimated from unlabeled data, using EM algorithm or Markov chain Monte–Carlo (MCMC) method. Square-error partitional clustering can be viewed as a particular case of mixture decomposition method. The description of $k$-means algorithm and the EM algorithm is given in Section 8.2.3.

### 1.4.4 Classifier Combination

Wolpert's "No Free Lunch" theorem states that there is no overall optimal classification rule [190]: every classifier could be a best choice for certain classification problems. Nevertheless, classifiers can be combined to get a more accurate classification decision at the expense of increased complexity. The motivations of combining classifiers are [191]

- to minimize the effect of the worst classifier by averaging several classifiers;
- to improve the performance of the best individual classifier;
- to avoid local minima and thereby stabilize and improve the best single classifier result.

There are three basic types of combining schemes [164]: (1) In parallel architecture, individual classifiers are invoked independently and their outputs are combined. (2) In cascading architecture [192], individual classifiers are invoked in a sequential manner.

The next classifier is trained in order to correct the errors of the previous classifier. (3) In hierarchical architecture, individual classifiers are organized as tree structure or DAG (directed acyclic graph) structure [193].

We will describe two methods of classifier combination here: AdaBoost and random forest. AdaBoost or adaptive boosting, proposed by Freund and Schapire in Reference [183], trains classifiers in a cascading architecture: after the training of the current classifier, the misclassified patterns are given more weightage in order to be considered more important in the training of the classifier that follows next in the sequence. In Reference [194], Schapire showed in his original work that, a combination of weak classifiers can be boosted to an arbitrarily strong model. Boosting has been widely used in conjunction with other learning algorithms to improve the accuracy. The details of AdaBoost and EAdaBoost algorithms are given in Section 10.2.4.

Random forest [195] is constructed by a multitude of decision trees at training time. Each tree is trained on a bootstrapped sample from the original data. Each node is split using the best among a subset of predictors randomly chosen at that node, rather than using the best split among all variables. Random forest runs fast and is able to deal with unbalanced and missing data. For a detailed review on combined classifiers, the readers may prefer to Kuncheva's paper [187].

### 1.4.5 Frontiers of Pattern Classification for Biomedical Image Understanding

Neural networks [196] and *k*-means [197] clustering have been used for automatic classification of tuberculosis bacteria in sputum smear microscopic images. In Reference [198], a boosted Bayesian multiresolution classifier was proposed for prostate cancer detection from digitized needle biopsies.

Medical X-ray image classification methods include applying Bayesian rule on shape features [199], local binary patterns (LBPs), and random forest [200], merging scheme-based SVM [201]. The methods for the classification of mammographic masses include using gradient and texture features [202], binary decision tree [203], and neural networks [204]. A feature extraction technique that is able to detect signs of cancer development in mammograms taken 10–18 months prior to cancer detection was presented in Reference [205]. Wei et al. [206] tested several machine learning methods for automated classification of clustered microcalcifications in mammograms: SVM, kernel Fisher discriminant, relevance vector machine, and committee machines (ensemble averaging and AdaBoost).

Recent works on MRI brain segmentation include adaptive mean shift clustering [207], autocontext in discriminative models [208], Bayesian brain tissue classification, and random forest based lesion classification [209]. Blind source separation has been used for the estimation of tissue intensity distribution in MR images [210]. SVM is still a popular method for classification of MR breast lesions [211, 212]. Fuzzy clustering has been used for classification of myocardial infarct in delayed enhancement MRI [213].

For breast cancer detection in 3D ultrasound images, Tan et al. [214] used neural network classifiers to obtain a likelihood map of potential abnormality in the initial detection stage. Region classification was performed using an ensemble of neural networks, a SVM, a KNN, a linear discriminant, and a gentle boost classifier. A recent survey on breast cancer detection and classification using ultrasound images can be found in Reference [215]. For prostate cancer detection in transrectal ultrasound images, Moradi et al. [216] used an extension to the SVM classification approach and a hybrid feature vector combining radio frequency (RF) time series, RF spectral features, and texture feature. For the same application, a multifeature kernel classification model based on generalized discriminant analysis was proposed in Reference [217].

In Chapter 8, basic pattern classification techniques used in biomedical image understanding are summarized, including Bayesian decision theory, SVM, *k*-means clustering, and EM algorithm. As an illustration, a framework comprising blood smear analysis, malarial infection detection, and grading from blood cell images is presented in detail. For detection of good working areas (GWAs), object segmentation and clump splitting are carried out using image processing methods. SVM is used to classify the images using the area of a clump and the number of cells it contains. In dual-model-guided image segmentation and recognition, shape and color models are combined to improve the segmentation accuracy. A region-color-based Bayesian classifier is adopted for shape-valid region classification. Finally, malarial infection and staging are integrated into a four-class SVM to classify the regions segmented earlier.

In Chapter 9, liver tumor segmentation under a hybrid SVM framework and liver tumor characterization by content-based image retrieval are discussed. The three-stage hybrid SVM scheme involves a trained one-class support vector classifier (OSVC) for presegmentation, a boosting tool employed to automatically generate negative samples, and binary support vector classifier (BSVC) training and classification for final segmentation. The good recognition capability of OSVC and the good discrimination capability of BSVC are utilized in this hybrid scheme and their disadvantages are suppressed.

In Chapter 10, several classification models based on KNN are applied in computerized Gemstone spectral imaging computed tomography (GSI-CT) data analysis, contributing to the N grading of lymph node metastasis in gastric cancer. The related feature selection, metric learning, and classification methods are introduced. Feature selection methods include mRMR and SFS algorithms. Metric learning methods include PCA and Fisher discriminant analysis. Classification methods include KNN, AdaBoost and EAdaBoost algorithms.

## 1.5 KNOWLEDGE-BASED SYSTEMS

### 1.5.1 Semantic Interpretation and Knowledge-Based Systems

Over the past few decades, researchers in image processing, computer vision, and AI have worked hard to develop intelligent vision systems that are capable of performing tasks that human vision can handle. Although a lot of progresses have been made in detection, recognition, reconstruction, and so on [218], current state-of-the-art intelligent vision systems are not yet comparable to human vision in terms of understanding high-level semantic meanings of visual information. Intelligent semantic interpretation of visual information is still an opening research problem. In another aspect, as early as in the 1970s, researchers in AI realized that *knowledge* is essential for intelligence [219, 220]. Knowledge-based systems (KBSs) emerged since 1970s, which reason and use knowledge to solve complex problems [219, 221]. The core components of KBS include knowledge base, knowledge acquisition mechanisms, and inference mechanisms [221]. Expert systems [222] and case-based reasoning systems [223] are typical types of KBS. Accordingly, how to acquire knowledge and represent large amounts of knowledge as knowledge base to be easily used in computer programs started to become the research focus of AI field in the 1970s [224, 225]. Over the past 40 years, with the development of knowledge engineering, data mining, and machine learning techniques, knowledge acquisition has evolved from human manual input to large-scale data-driven knowledge discovery [226–228]. Knowledge representation has evolved from explicit rule-based, frame-based representations, ontology representation, to complex statistical models [224, 225, 229].

### 1.5.2 Knowledge-Based Vision Systems

Together with the development of knowledge-based AI systems, large numbers of generic or domain-specific knowledge-based vision systems have been developed [230–232]. These systems are characterized in terms of their domains or visual tasks, the type of knowledge being used, the way knowledge is acquired, the way knowledge is represented, and the way knowledge is used in inference in visual information interpretation process. Detailed reviews can be found in References [233–235].

Early knowledge-based vision systems developed in the 1980s combine expert system tools together with low-level image processing for visual interpretation [230–232]. In these early systems, knowledge is acquired from human experts' input and is represented as explicit rules or schemas. Rule-based or schema reasoning system controls the process of image processing and interpretation.

Since the 1990s, as research focus shifted to more difficult tasks, it became more and more clear that knowledge acquired from human expert input is inadequate as such knowledge tends to be qualitative and imprecise. On the other hand, with the development of digital storage technology, larger and larger amount of data was gathered in daily practice. This led to the development of early data mining or machine learning techniques aimed to automatically extract knowledge from data collection using statistical modeling [228, 236, 237]. Together with this evolution in knowledge acquisition, implicit knowledge representation and inference based on statistical techniques such as principle component analysis (PCA) [238, 239], linear discriminant analysis (LDA) [240], and Bayesian models [241] started to become popular since late 1990s. This kind of techniques effectively models intraclass variations as *a priori* knowledge and facilitates high-level semantic interpretation.

In the recent decade, many advanced machine learning techniques such as graphical models (e.g., Bayesian network (BN) [242, 243], conditional random fields

**TABLE 1.5 Research Trend in Knowledge-Based Vision Systems**

| | |
|---|---|
| Early years–1980s | Expert systems [220], rule-based/schema-based, and so on for knowledge representation; manual input for knowledge acquisition [230–232] |
| 1990s | Systems using statistical modeling (PCA, LDA, and ASM) techniques for knowledge acquisition, representation, and inference [238–241] |
| 2000–current | Systems using advanced machine learning techniques (e.g., Bayesian networks, and CRFs) for knowledge acquisition, representation, and inference [242–245] |
| Current and the future | Systems performing large-scale data-driven knowledge discovery [248] |

(CRFs) [244, 245]), latent semantic models [246], and deep belief networks [247] have been used in complex implicit knowledge modeling. As the field is moving toward big data era, we can expect more and more large-scale data-driven knowledge acquisition or discovery algorithms to emerge [248] (see Table 1.5).

### 1.5.3 Knowledge-Based Vision Systems in Biomedical Image Analysis

In the domain of biomedical image analysis, knowledge is extremely crucial for the success of intelligent vision systems since even a human domain expert needs intensive training to obtain knowledge for interpreting biomedical images. Compared to generic knowledge-based vision systems, knowledge acquisition and representation in biomedical image analysis are more complex and difficult, which require close collaborations between computer scientists and biomedical experts.

Knowledge introduced into biomedical image analysis can be mainly classified into the following two types: conceptual knowledge and domain knowledge. The first type – conceptual knowledge is related to primitive visual features in image interpretation process. It includes information about the appearance and geometrical configuration of objects in biomedical images. Such knowledge was often represented as rules, schemas, or ontologies. Since 1990s, statistical models such as AAM [28], SSM [58], and atlas [249] have become popular for conceptual knowledge representation. Conceptual knowledge has been extensively applied to biomedical image analysis tasks such as object segmentation [250, 251], pathology detection [252], and image retrieval [253]. The second type – domain knowledge is about semantic biomedical knowledge related to diagnosis. This includes knowledge on anatomy, pathology, histology, biology, biochemistry, and so on. Unified medical language system (UMLS) [254] is a widely adopted system for standard domain terminology representation. Domain knowledge, often combined together with conceptual knowledge, has been used to guide a variety of medical image analysis tasks [255–257].

### 1.5.4 Frontiers of Knowledge-Based Systems

With the current rapid advancement of data mining, machine learning, and computer vision techniques, we can foresee that future intelligent vision systems will be built upon knowledge discovered from large-scale data and progressing toward semantic interpretation, which approaches the capability of human vision. Knowledge-based approach seems to be a promising approach for achieving *visual intelligence*. In biomedical image analysis, with the fast development of bioimaging techniques, a lot of future research efforts are needed to transfer the vast amounts of expert human knowledge to computer knowledge base in intelligent computer-assisted diagnosis (CAD) systems.

Chapter 11 provides an extensive introduction and review of how knowledge is represented and introduced in biomedical image analysis. The relationships among data, information, and knowledge are elaborated. Techniques of explicit and implicit forms of knowledge representation are summarized. The chapter also reviews four major frameworks of knowledge-based vision systems in biomedical image analysis: multiscale framework, deformable oriented framework, Bayesian network framework, and ontology-based framework. This chapter provides an insight on how knowledge is represented and integrated in biomedical image understanding systems.

Chapter 12 demonstrates a particular use of knowledge for ocular image analysis. It provides a review of ASM and introduces its application in contour detection of anatomical structures. The chapter gives a background in 2D deformable models and introduces point distribution model (PDM), ASM, and its variants. The chapter also includes two specific applications: boundary detection of optic disc and detection of lens structure. In contrast to Chapter 11, this chapter illustrates how object shape, a specific form of prior knowledge is represented as deformable model and incorporated in intelligent vision system to detect object contour.

## REFERENCES

[1] J. K. Tsotos. Image understanding. In S. C. Shapiro, editor, *Encyclopedia of Artificial Intelligence*. John Wiley & Sons, Inc., New York, 1987.

[2] D. L. Pham, C. Xu, and J. L. Prince. Current methods in medical image segmentation. *Annual Review of Biomedical Engineering*, 2:315–337, 2000.

[3] N. Sharma and L. M. Aggarwal. Automated medical image segmentation techniques. *Journal of Medical Physics*, 35(1):3–14, 2010.

[4] M. Rastgarpour and J. Shanbehzadeh. Application of AI techniques in medical image segmentation and novel categorization of available methods and tools. In *Proceedings of the International MultiConference of Engineers and Computer Scientists*, volume I, 2011.

[5] C. Jung and C. Kim. Segmenting clustered nuclei using H-minima transform-based marker extraction and contour parameterization. *IEEE Transactions on Biomedical Engineering*, 57(10):2600–2604, 2010.

[6] F. Cloppet and A. Boucher. Segmentation of complex nucleus configurations in biological images. *Pattern Recognition Letters*, 31(8):755–761, 2010.

[7] J. Cheng and J. C. Rajapakse. Segmentation of clustered nuclei with shape markers and marking function. *IEEE Transactions on Biomedical Engineering*, 56(3):741–748, 2009.

[8] R. Kumar and A. A. M. A comparative study of image segmentation using edge-based approach. *International Journal of Mathematics*, 7(3):18–22, 2013.

[9] R. Adams and L. Bischof. Seeded region growing. *IEEE Transactions on Pattern Analysis and Machine Intelligence*, 16(6):641–647, 1994.

[10] J. Anquez, E. D. Angelini, and I. Bloch. Automatic segmentation of head structures on fetal MRI. In *Proceedings of the Sixth IEEE International Conference on Symposium on Biomedical Imaging: From Nano to Macro*, Piscataway, NJ, USA, 2009. IEEE Press.

[11] G. N. Harikrishna Rai and T. R. Gopalakrishnan Nair. Gradient based seeded region grow method for CT angiographic image segmentation. In *Proceedings of IEEE Conference on Computer Vision and Pattern Recognition*, 2010.

[12] L. Zhu, Y. Gao, V. Appia, A. Yezzi, C. Arepalli, T. Faber, A. Stillman, and A. Tannenbaum. Automatic delineation of the myocardial wall from CT images via shape segmentation and variational region growing. *IEEE Transactions on Biomedical Engineering*, 60(10):2887–2895, 2013.

[13] H. Zhang, A. C. Berg, M. Maire, and J. Malik. SVM-KNN: discriminative nearest neighbor classification for visual category recognition. In *Proceedings of IEEE Conference on Computer Vision and Pattern Recognition*, volume 2, pages 2126–2136, 2006.

[14] K. Fukunage and P. M. Narendra. A branch and bound algorithm for computing K-nearest neighbors. *IEEE Transactions on Computers*, 24(7):750–753, 2006.

[15] R. O. Duda, P. E. Hart, and D. G. Stork. *Pattern Classification*. Wiley-Interscience, 2nd edition, 2000.

[16] O. Chapelle. *Support vector machines: induction principles, adaptive tuning and prior knowledge*. Doctoral dissertation, LIP6, 2003.

[17] L. Devroye, L. Györfi, and G. Lugosi. *A Probabilistic Theory of Pattern Recognition*. Springer, 1997.

[18] J. MacQueen. Some methods for classification and analysis of multivariate observations. In *Proceedings of the Fifth Berkeley Symposium on Mathematical Statistics and Probability*, volume 1, pages 281–297, 1967.

[19] J. C. Dunn. A fuzzy relative of the isodata process and its use in detecting compact well-separated clusters. *Journal of Cybernetics*, 3(3):32–57, 1973.

[20] J. C. Bezdek. *Pattern Recognition with Fuzzy Objective Function Algoritms*. Plenum Press, New York, 1981.

[21] D. J. C. MacKay. *Information Theory, Inference, and Learning Algorithms*. Cambridge University Press, 2003.

[22] M. Kass, A. Witkin, and D. Terzopoulos. Snakes: active contour models. *International Journal of Computer Vision*, 1(4):321–331, 1988.

[23] S. Osher and J. A. Sethian. Fronts propagating with curvature dependent speed: algorithms based on Hamilton-Jacobi formulations. *Journal of Computational Physics*, 79(1):12–49, 1988.

[24] V. Caselles, R. Kimmel, and G. Sapiro. Geodesic active contours. *International Journal of Computer Vision*, 22(1):61–79, 1997.

[25] R. Malladi, J. A. Sethian, and B. C. Vemuri. Shape modeling with front propagation: a level set approach. *IEEE Transactions on Pattern Analysis and Machine Intelligence*, 17:158–175, 1995.

[26] D. Mumford and J. Shah. Optimal approximations by piecewise smooth functions and associated variational problems. *Communications on Pure and Applied Mathematics*, 42(5):577–685, 1989.

[27] T. F. Cootes, C. J. Taylor, D. H. Cooper, and J. Graham. Active shape models - their training and application. *Computer Vision and Image Understanding*, 61(1):38–59, 1995.

[28] T. F. Cootes, G. J. Edwards, and C. J. Taylor. Active appearance models. *IEEE Transactions on Pattern Analysis and Machine Intelligence*, 23(6):681–685, 2001.

[29] S. K. Michopoulou, L. Costaridou, E. Panagiotopoulos, R. D. Speller, G. Panayiotakis, and A. Todd-Pokropek. Atlas-based segmentation of degenerated lumbar intervertebral discs from MR images of the spine. *IEEE Transactions on Biomedical Engineering*, 56(9):2225–2231, 2009.

[30] F. van der Lijn, M. de Bruijne, S. Klein, T. den Heijer, Y. Y. Hoogendam, A. van der Lugt, M. M. B. Breteler, and W. J. Niessen. Automated brain structure segmentation based on atlas registration and appearance models. *IEEE Transactions on Medical Imaging*, 31(2):276–286, 2012.

[31] A. A. Farag, A. El-Baz, and G. L. Gimel’farb. Precise segmentation of multimodal images. *IEEE Transactions on Image Processing*, 15(4):952–968, 2006.

[32] M. Droske and M. Rumpf. Multiscale joint segmentation and registration of image morphology. *IEEE Transactions on Pattern Analysis and Machine Intelligence*, 29(12):2181–2194, 2007.

[33] S. Ahmed, K. M. Iftekharuddin, and A. Vossough. Efficacy of texture, shape, and intensity feature fusion for posterior-fossa tumor segmentation in MRI. *IEEE Transactions on Information Technology in Biomedicine*, 15(2):206–213, 2011.

[34] T. Shen, Y. Zhu, X. Huang, J. Huang, D. Metaxas, and L. Axel. Active volume models with probabilistic object boundary prediction module. In *Proceedings of the Eleventh International Conference on Medical Image Computing and Computer-Assisted Intervention*, pages 331–341. Springer-Verlag, 2008.

[35] L. Grady. Random walks for image segmentation. *IEEE Transactions on Pattern Analysis and Machine Intelligence*, 28(11):1768–1783, 2006.

[36] A. Protiere and G. Sapiro. Interactive image segmentation via adaptive weighted distances. *IEEE Transactions on Image Processing*, 16(4):1046–1057, 2007.

[37] O. Veksler. Star shape prior for graph-cut image segmentation. In *Proceedings of the European Conference on Computer Vision*, pages 454–467, 2008.

[38] S. Vicente, V. Kolmogorov, and C. Rother. Graph cut based image segmentation with connectivity priors. In *Proceedings of IEEE Conference on Computer Vision and Pattern Recognition*, pages 1–8, 2008.

[39] K. Ciesielski, J. K. Udupa, P. K. Saha, and Y. Zhuge. Iterative relative fuzzy connectedness for multiple objects with multiple seeds. *Computer Vision and Image Understanding*, 107(3):160–182, 2007.

[40] J. K. Udupa and S. Samarasekera. Fuzzy connectedness and object definition: theory, algorithms, and applications in image segmentation. *CVGIP: Graphical Model and Image Processing*, 58(3):246–261, 1996.

[41] L. Vincent and P. Soille. Watersheds in digital spaces: an efficient algorithm based on immersion simulations. *IEEE Transactions on Pattern Analysis and Machine Intelligence*, 13(6):583–598, 1991.

[42] M. Hatt, C. Cheze-Le Rest, A. Turzo, C. Roux, and D. Visvikis. A fuzzy locally adaptive Bayesian segmentation approach for volume determination in pet. *IEEE Transactions on Medical Imaging*, 28(6):881–893, 2009.

[43] F. Destrempes, J. Meunier, M.-F. Giroux, G. Soulez, and G. Cloutier. Segmentation of plaques in sequences of ultrasonic B-mode images of carotid arteries based on motion estimation and a Bayesian model. *IEEE Transactions on Biomedical Engineering*, 58(8):2202–2211, 2011.

[44] M. Pereyra, N. Dobigeon, H. Batatia, and J.-Y. Tourneret. Segmentation of skin lesions in 2-D and 3-D ultrasound images using a spatially coherent generalized Rayleigh mixture model. *IEEE Transactions on Medical Imaging*, 31(8):1509–1520, 2012.

[45] G. Grange, J. Anquez, E. D. Angelini, and I. Bloch. Automatic segmentation of antenatal 3-D ultrasound images. *IEEE Transactions on Biomedical Engineering*, 60(5):1388–1400, 2013.

[46] J. L. Marroquín, B. C. Vemuri, S. Botello, F. Calderón, and A. Fernández-Bouzas. An accurate and efficient Bayesian method for automatic segmentation of brain MRI. *IEEE Transactions on Medical Imaging*, 21(8):934–945, 2002.

[47] C. Jung, C. Kim, S. W. Chae, and S. Oh. Unsupervised segmentation of overlapped nuclei using Bayesian classification. *IEEE Transactions on Biomedical Engineering*, 57(12):2825–2832, 2010.

[48] Z. Ji, Y. Xia, Q.-S. Sun, Q. Chen, D.-S. Xia, and D. D. Feng. Fuzzy local Gaussian mixture model for brain MR image segmentation. *IEEE Transactions on Information Technology in Biomedicine*, 16(3):339–347, 2012.

[49] X. Liu, D. L. Langer, M. A. Haider, Y. Yang, M. N. Wernick, and I. S. Yetik. Prostate cancer segmentation with simultaneous estimation of Markov random field parameters and class. *IEEE Transactions on Medical Imaging*, 28(6):906–915, 2009.

[50] Y. Zhang, M. Brady, and S. Smith. Segmentation of brain MR images through a hidden Markov random field model and the expectation-maximization algorithm. *IEEE Transactions on Medical Imaging*, 20(1):45–57, 2001.

[51] J. Wu and A. C. S. Chung. A segmentation model using compound Markov random fields based on a boundary model. *IEEE Transactions on Image Processing*, 16(1):241–252, 2007.

[52] S. Zhou, W. Chen, F. Jia, Q. Hu, Y. Xie, M. Chen, and J. Wu. Segmentation of brain magnetic resonance angiography images based on MAP-MRF with multi-pattern neighborhood system and approximation of regularization coefficient. *Medical Image Analysis*, 17(8):1220–1235, 2013.

[53] S. Kadoury, H. Labelle, and N. Paragios. Spine segmentation in medical images using manifold embeddings and higher-order MRFS. *IEEE Transactions on Medical Imaging*, 32(7):1227–1238, 2013.

[54] G. Xiao, M. Brady, J. A. Noble, and Y. Zhang. Segmentation of ultrasound B-mode images with intensity inhomogeneity correction. *IEEE Transactions on Medical Imaging*, 21(1):48–57, 2002.

[55] V. Grau, J. C. Downs, and C. Burgoyne. Segmentation of trabeculated structures using an anisotropic Markov random field: application to the study of the optic nerve head in glaucoma. *IEEE Transactions on Medical Imaging*, 25(3):245–255, 2006.

[56] S. Arslan, T. Ersahin, R. Cetin-Atalay, and C. Gunduz-Demir. Attributed relational graphs for cell nucleus segmentation in fluorescence microscopy images. *IEEE Transactions on Medical Imaging*, 32(6):1121–1131, 2013.

[57] T. Shen, H. Li, and X. Huang. Active volume models for medical image segmentation. *IEEE Transactions on Medical Imaging*, 30(3):774–791, 2011.

[58] T. Heimann and H.-P. Meinzer. Statistical shape models for 3D medical image segmentation: a review. *Medical Image Analysis*, 13(4):543–563, 2009.

[59] H. Wang, J. W. Suh, S. R. Das, J. B. Pluta, C. Craige, and P. A. Yushkevich. Multi-atlas segmentation with joint label fusion. *IEEE Transactions on Pattern Analysis and Machine Intelligence*, 35(3):611–623, 2013.

[60] W. Bai, W. Shi, D. P. O'Regan, T. Tong, H. Wang, S. Jamil-Copley, N. S. Peters, and D. Rueckert. A probabilistic patch-based label fusion model for multi-atlas segmentation with registration refinement: application to cardiac MR images. *IEEE Transactions on Medical Imaging*, 32(7):1302–1315, 2013.

[61] H. Ji, J. He, X. Yang, R. Deklerck, and J. Cornelis. ACM-based automatic liver segmentation from 3-D CT images by combining multiple atlases and improved mean-shift techniques. *IEEE Journal of Biomedical and Health Informatics*, 17(3):690–698, 2013.

[62] D. Yang, J. Zheng, A. Nofal, J. O. Deasy, and I. M. El Naqa. Techniques and software tool for 3D multimodality medical image segmentation. *Journal of Radiation Oncology Informatics*, 1(1):1–21, 2009.

[63] A. S. El-Baz, U. R. Acharya, M. Mirmehdi, and J. S. Suri. *Multi Modality State-of-the-Art Medical Image Segmentation and Registration Methodologies*. Springer, 2011.

[64] Y. Y. Zhu. *Towards more desirable segmentation via user interactions*. PhD thesis, Computer Engineering, Lehigh University, 2013.

[65] P. Fua and C. Brechbuhler. Imposing hard constraints on soft snakes. In *Proceedings of the European Conference on Computer Vision*, pages 495–506, 1996.

[66] T. Mcinerney and D. Terzopoulos. T-snakes: topology adaptive snakes. *Medical Image Analysis*, 18(10):840–845, 1999.

[67] Y. Boykov, O. Veksler, and R. Zabih. Fast approximate energy minimization via graph cuts. In *Proceedings of IEEE International Conference on Computer Vision*, pages 377–384, 1999.

[68] A. Sotiras, D. Christos, and N. Paragios. Deformable medical image registration: a survey. *IEEE Transactions on Medical Imaging*, 32(7):1153–1190, 2013.

[69] L. G. Brown. A survey of image registration techniques. *ACM Computing Surveys*, 24:325–376, 1992.

[70] C. R. Maurer Jr. and J. M. Fitzpatrick. A review of medical image registration. *Interactive Imageguided Neurosurgery*, pages 17–44, American Association of Neurological Surgeons, Parkridge, IL, 1993.

[71] J. B. A. Maintz and M. A. Viergever. A survey of medical image registration. *Medical Image Analysis*, 2(1):1–36, 1998.

[72] D. L. G. Hill, P. G. Batchelor, M. Holden, and D. J. Hawkes. Medical image registration. *Physics in Medicine and Biology*, 46(3):R1–45, 2001.

[73] B. Zitová and J. Flusser. Image registration methods: a survey. *Image and Vision Computing*, 21:977–1000, 2003.

[74] T. Mäkelä, P. Clarysse, O. Sipilä, N. Pauna, Q.-C. Pham, T. Katila, and I. E. Magnin. A review of cardiac image registration methods. *IEEE Transactions on Medical Imaging*, 21(9):1011–1021, 2002.

[75] A. A. Moghe and J. Singhai. Article: image registration: a review of elastic registration methods applied to medical imaging. *International Journal of Computer Applications*, 70(7):6–11, 2013.

[76] V. Tavakoli and A. A. Amini. A survey of shaped-based registration and segmentation techniques for cardiac images. *Computer Vision and Image Understanding*, 117(9):966–989, 2013.

[77] V. R. S Mani and Dr. S. Rivazhagan. Survey of medical image registration. *Journal of Biomedical Engineering and Technology*, 1(2):8–25, 2013.

[78] F. Graf, H.-P. Kriegel, M. Schubert, S. Pölsterl, and A. Cavallaro. 2D image registration in CT images using radial image descriptors. In *Proceedings of International Conference on Medical Image Computing and Computer Assist Intervention (Pt 2)*, pages 607–614, 2011.

[79] J. B. A. Maintz, P. A. van den Elsen, and M. A. Viergever. 3D multimodality medical image registration using morphological tools. *Image and Vision Computing*, 19((1-2)):53–62, 2001.

[80] D. Jaffray, P. Kupelian, T. Djemil, and R. M. Macklis. Review of image-guided radiation therapy. *Expert Review of Anticancer Therapy*, 7(1):89–103, 2007.

[81] T. M. Peters and K. R. Cleary. *Image-Guided Interventions: Technology and Applications*. SpringerLink Engineering, Springer, 2008.

[82] P. Markelj, D. Tomaževič, B. Likar, and F. Pernuš. A review of 3D/2D registration methods for image-guided interventions. *Medical Image Analysis*, 16(3):642–661, 2012.

[83] J. B. West, J. M. Fitzpatrick, S. A. Toms, C. R. Maurer Jr., and R. J. Maciunas. Fiducial point placement and the accuracy of point-based, rigid body registration. *Neurosurgery*, 48(4):810–817, 2001.

[84] L. Lemieux, N. D. Kitchen, S. W. Hughes, and D. G. T. Thomass. Voxel-based localization in frame-based and frameless stereotaxy and its accuracy. *Medical Physics*, 21(8):1301–1310, 1994.

[85] K. Rohr, M. Fornefett, and H. S. Stiehl. Spline-based elastic image registration: integration of landmark errors and orientation attributes. *Computer Vision and Image Understanding*, 90(2):153–168, 2003.

[86] E. De Castro and C. Morandi. Registration of translated and rotated images using finite Fourier transforms. *IEEE Transactions on Pattern Analysis and Machine Intelligence*, 9(5):700–703, 1987.

[87] P. J. Besl and N. D. McKay. A method for registration of 3-D shapes. *IEEE Transactions on Pattern Analysis and Machine Intelligence*, 14(2):239–256, 1992.

[88] B. S. Reddy and B. N. Chatterji. An FFT-based technique for translation, rotation, and scale-invariant image registration. *IEEE Transactions on Image Processing*, 5(8):1266–1271, 1996.

[89] F. L. Bookstein. Principal warps: Thin-plate splines and the decomposition of deformations. *IEEE Transactions on Pattern Analysis and Machine Intelligence*, 11(6):567–585, 1989.

[90] K. Rohr, H. S. Stiehl, R. Sprengel, T. M. Buzug, J. Weese, and M. H. Kuhn. Landmark-based elastic registration using approximating thin-plate splines. *IEEE Transactions on Pattern Analysis and Machine Intelligence*, 20(6):526–534, 2001.

[91] A. A. Goshtasby. *2-D and 3-D Image Registration: for Medical, Remote Sensing, and Industrial Applications*. Wiley-Interscience, 2005.

[92] A. P. Dhawan. *Medical Image Analysis*, *IEEE Press Series on Biomedical Engineering*. Wiley, 2011.

[93] C. Broit. *Optimal registration of deformed images*. Doctoral dissertation, University of Pennsylvania, Philadelphia, 1981.

[94] R. Bajcsy and S. Kovačič. Multiresolution elastic matching. *Computer Vision, Graphics, and Image Processing*, 46(1):1–21, 1989.

[95] S. A. Butt, R. Acharya, C. Sibata, and K. H. Shin. Surface matching of multimodality image volumes by a fuzzy elastic registration technique. *Computerized Medical Imaging and Graphics*, 22(1):13–23, 1998.

[96] D. Shen and C. Davatzikos. Hammer: hierarchical attribute matching mechanism for elastic registration. *IEEE Transactions on Medical Imaging*, 21:1421–1439, 2002.

[97] G. E. Christensen, R. D. Rabbitt, and M. I. Miller. Deformable templates using large deformation kinematics. *IEEE Transactions on Image Processing*, 5(10):1435–1447, 1996.

[98] M. Bro-Nielsen and C. Gramkow. Fast fluid registration of medical images. In *Proceedings of the Fourth International Conference on Visualization in Biomedical Computing*, pages 267–276, 1996.

[99] J. P. Thirion. Image matching as a diffusion process: an analogy with Maxwell's demons. *Medical Image Analysis*, 2(3):243–260, 1998.

[100] H. Lester and S. R. Arridge. A survey of hierarchical non-linear medical image registration. *Pattern Recognition*, 32(1):129–149, 1999.

[101] M. F. Beg, M. I. Miller, A. Trouvé, and L. Younes. Computing large deformation metric mappings via geodesic flows of diffeomorphisms. *International Journal of Computer Vision*, 61(2):139–157, 2005.

[102] J. Glaunes, A. Trouvé, and L. Younes. Diffeomorphic matching of distributions: a new approach for unlabelled point-sets and sub-manifolds matching. In *Proceedings of IEEE International Conference on Computer Vision and Pattern Recognition*, pages 712–718, 2004.

[103] J. Ashburner. A fast diffeomorphic image registration algorithm. *NeuroImage*, 38(1):95–113, 2007.

[104] G. Janssens, L. Jacques, J. O. de Xivry, X. Geets, and B. Macq. Diffeomorphic registration of images with variable contrast enhancement. *Journal of Biomedical Imaging*, 2011(3):1–12, 2011.

[105] M. Holden. A review of geometric transformations for nonrigid body registration. *IEEE Transactions on Medical Imaging*, 27(1):111–128, 2008.

[106] W. R. Crum, T. Hartkens, and D. L. Hill. Non-rigid image registration: theory and practice. *British Journal of Radiology*, 77:S140–S153, 2004.

[107] D. Rueckert, L. I. Sonoda, C. Hayes, D. L. G. Hill, M. O. Leach, and D. J. Hawkes. Nonrigid registration using free-form deformations: application to breast MR images. *IEEE Transactions on Medical Imaging*, 18:712–721, 1999.

[108] D. Mattes, D. R. Haynor, H. Vesselle, T. K. Lewellen, and W. Eubank. Pet-CT image registration in the chest using free-form deformations. *IEEE Transactions on Medical Imaging*, 22(1):120–128, 2003.

[109] A. F. Frangi, D. Rueckert, J. A. Schnabel, and W. J. Niessen. Automatic construction of multiple-object three-dimensional statistical shape models: application to cardiac modelling. *IEEE Transactions on Medical Imaging*, 21(9):1151–1166, 2002.

[110] C. Studholme, V. Cardenas, A. Maudsley, and M. Weiner. An intensity consistent filtering approach to the analysis of deformation tensor derived maps of brain shape. *NeuroImage*, 19(4):1638–1649, 2003.

[111] C. Ó. S. Sorzano, P. Thévenaz, and M. Unser. Elastic registration of biological images using vector-spline regularization. *IEEE Transactions on Biomedical Engineering*, 52(4):652–663, 2005.

[112] D. L. Wilson, D. Royston, J. A. Noble, and J. V. Byrne. Determining X-ray projections for coil treatments of intracranial aneurysms. *IEEE Transactions on Medical Imaging*, 18(10):973–980, 1999.

[113] A. Yilmaz, O. Javed, and M. Shah. Object tracking: a survey. *ACM Computing Surveys (CSUR)*, 38(4):1–45, 2006.

[114] Y. Saeys, I. Inza, and P. Larra naga. A review of feature selection techniques in bioinformatics. *Bioinformatics*, 23(19):2507–2517, 2007.

[115] A. M. Jacob and J. Anitha. Inspection of various object tracking techniques. *International Journal of Engineering and Innovative Technology*, 2(6):118–124, 2012.

[116] T. Chen, X. Wang, S. Chung, D. Metaxas, and L. Axel. Automated 3D motion tracking using Gabor filter bank, robust point matching, and deformable models. *IEEE Transactions on Medical Imaging*, 29(1):1–11, 2010.

[117] L. Yang, B. Georgescu, Y. Zheng, Y. Wang, P. Meer, and D. Comaniciu. Prediction based collaborative trackers (PCT): a robust and accurate approach toward 3D medical object tracking. *IEEE Transactions on Medical Imaging*, 30(11):1921–1932, 2011.

[118] C. Veenman, M. Reinders, and E. Backer. Resolving motion correspondence for densely moving points. *IEEE Transactions on Pattern Analysis and Machine Intelligence*, 23(1):54–72, 2001.

[119] D. Serby, S. Koller-Meier, and L. V. Gool. Probabilistic object tracking using multiple features. In *Proceedings of IEEE International Conference of Pattern Recognition*, pages 184–187, 2004.

[120] D. Comaniciu, V. Ramesh, and P. Meer. Kernel-based object tracking. *IEEE Transactions on Pattern Analysis and Machine Intelligence*, 25:564–575, 2003.

[121] A. Yilmaz, X. Li, and M. Shah. Contour based object tracking with occlusion handling in video acquired using mobile cameras. *IEEE Transactions on Pattern Analysis and Machine Intelligence*, 26(11):1531–1536, 2004.

[122] A. Sundaresan and R. Chellappa. Multi-camera tracking of articulated human motion using motion and shape cues. *IEEE Transactions on Image Processing*, 18(9):2114–2126, 2009.

[123] D. Ballard and C. Brown. *Computer Vision*. Prentice-Hall, 1982.

[124] A. Ali and J. Aggarwal. Segmentation and recognition of continuous human activity. In *IEEE Workshop on Detection and Recognition of Events in Video*, pages 28–35, 2001.

[125] G. Paschos. Perceptually uniform color spaces for color texture analysis: an empirical evaluation. *IEEE Transactions on Image Processing*, 10:932–937, 2001.

[126] K. Bowyer, C. Kranenburg, and S. Dougherty. Edge detector evaluation using empirical ROC curve. *Computer Vision and Image Understanding*, 84:77–103, 2001.

[127] B. Horn and B. Schunk. Determining optical flow. *Artificial Intelligence*, 17:185–203, 1981.

[128] B. D. Lucas and T. Kanade. An iterative image registration technique with an application to stereo vision. In *International Joint Conference on Artificial Intelligence*, pages 121–130, 1981.

[129] M. Black and P. Anandan. The robust estimation of multiple motions: parametric and piecewisesmooth flow fields. *Computer Vision and Image Understanding*, 63(1):75–104, 1996.

[130] R. Szeliski and J. Coughlan. Spline-based image registration. *International Journal of Computer Vision*, 16(1–3):185–203, 1997.

[131] J. Barron, D. Fleet, and S. Beauchemin. Performance of optical flow techniques. *International Journal of Computer Vision*, 12:43–77, 1994.

[132] R. Haralick, B. Shanmugam, and I. Dinstein. Textural features for image classification. *IEEE Transactions on Systems, Man, and Cybernetics*, 33(3):610–622, 1973.

[133] K. Laws. *Textured image segmentation*. PhD thesis, Electrical Engineering, University of Southern California, 1980.

[134] S. Mallat. A theory for multiresolution signal decomposition: the wavelet representation. *IEEE Transactions on Pattern Analysis and Machine Intelligence*, 11(7):674–693, 1989.

[135] H. Greenspan, S. Belongie, R. Goodman, P. Perona, S. Rakshit, and C. Anderson. Overcomplete steerable pyramid filters and rotation invariance. In *Proceedings of IEEE International Conference on Computer Vision and Pattern Recognition*, pages 222–228, 1994.

[136] D. Koller and M. Sahami. Toward optimal feature selection. In *Proceedings of the Thirteenth International Conference on Machine Learning*, pages 284–292, 1996.

[137] L. Yu and H. Liu. Efficient feature selection via analysis of relevance and redundancy. *Journal of Machine Learning Research*, 5:1205–1224, 2004.

[138] W. Siedelecky and J. Sklansky. On automatic feature selection. *International Journal of Pattern Recognition*, 2:197–220, 1988.

[139] D. Skalak. Prototype and feature selection by sampling and random mutation hill climbing algorithms. In *Proceedings of the Eleventh International Conference on Machine Learning*, pages 293–301, 1994.

[140] I. Inza, P. Larra naga, R. Etxebarria, and B. Sierra. Feature subset selection by Bayesian networks based optimization. *Artificial Intelligence*, 123(1–2):157–184, 2000.

[141] I. Guyon, J. Weston, S. Barnhill, and V. Vapnik. Gene selection for cancer classification using support vector machines. *Machine Learning*, 46(1–3):389–422, 2002.

[142] J. Weston, A. Elisseeff, B. Schoelkopf, and M. Tipping. Use of the zero-norm with linear models and kernel methods. *Journal of Machine Learning Research*, 3:1439–1461, 2003.

[143] V. Salari and I. K. Sethi. Feature point correspondence in the presence of occlusion. *IEEE Transactions on Pattern Analysis and Machine Intelligence*, 12(1):87–91, 1990.

[144] T. Broida and R. Chellappa. Estimation of object motion parameters from noisy images. *IEEE Transactions on Pattern Analysis and Machine Intelligence*, 8(1):90–99, 1986.

[145] Y. Bar-Shalom and T. Foreman. *Tracking and Data Association*. Academic Press Inc., 1988.

[146] R. L. Streit and T. E. Luginbuhl. Maximum likelihood method for probabilistic multi-hypothesis tracking. In *Proceedings of the International Society for Optical Engineering (SPIE)*, volume 2235, pages 394–405, 1994.

[147] J. Shi and C. Tomasi. Good features to track. In *Proceedings of IEEE International Conference on Computer Vision and Pattern Recognition*, pages 593–600, 1994.

[148] H. Tao, H. Sawhney, and R. Kumar. Object tracking with Bayesian estimation of dynamic layer representations. *IEEE Transactions on Pattern Analysis and Machine Intelligence*, 24(1):75–89, 2002.

[149] M. Black and A. Jepson. Eigentracking: robust matching and tracking of articulated objects using a view-based representation. *International Journal of Computer Vision*, 26(1):63–84, 1998.

[150] S. Avidan. Support vector tracking. In *Proceedings of IEEE International Conference on Computer Vision and Pattern Recognition*, pages 184–191, 2001.

[151] D. Huttenlocher, J. Noh, and W. Rucklidge. Tracking nonrigid objects in complex scenes. In *Proceedings of IEEE International Conference on Computer Vision*, pages 93–101, 1993.

[152] K. Sato and J. Aggarwal. Temporal spatio-velocity transform and its application to tracking and interaction. *Computer Vision and Image Understanding*, 96(2):100–128, 2004.

[153] J. Kang, I. Cohen, and G. Medioni. Object reacquisition using geometric invariant appearance model. In *Proceedings of International Conference on Pattern Recognition*, pages 759–762, 2004.

[154] M. Isard and A. Blake. Condensation - conditional density propagation for visual tracking. *International Journal of Computer Vision*, 29(1):5–28, 1998.

[155] M. Bertalmio, G. Sapiro, and G. Randall. Morphing active contours. *IEEE Transactions on Pattern Analysis and Machine Intelligence*, 22(7):733–737, 2000.

[156] R. Ronfard. Region based strategies for active contour models. *International Journal of Computer Vision*, 13(2):229–251, 1994.

[157] S. Zhu and A. Yuille. Region competition: unifying snakes, region growing, and Bayes/MDL for multiband image segmentation. *IEEE Transactions on Pattern Analysis and Machine Intelligence*, 18(9):884–900, 1996.

[158] N. Paragios and R. Deriche. Geodesic active regions and level set methods for supervised texture segmentation. *International Journal of Computer Vision*, 46(3):223–247, 2002.

[159] A. Elgammal, R. Duraiswami, D. Harwood, and L. Davis. Background and foreground modeling using nonparametric kernel density estimation for visual surveillance. In *Proceedings of the IEEE*, volume 90, pages 1151–1163, 2002.

[160] P. Fieguth and D. Terzopoulos. Color-based tracking of heads and other mobile objects at video frame rates. In *Proceedings of IEEE International Conference on Computer Vision and Pattern Recognition*, pages 21–27, 1997.

[161] G. Edwards, C. Taylor, and T. Cootes. Interpreting face images using active appearance models. In *Proceedings of International Conference on Face and Gesture Recognition*, pages 300–305, 1998.

[162] B. Mughadam and A. Pentland. Probabilistic visual learning for object representation. *IEEE Transactions on Pattern Analysis and Machine Intelligence*, 19(7):696–710, 1997.

[163] S. Watanabe. *Pattern Recognition: Human and Mechanical*. John Wiley & Sons, Inc., New York, NY, 1985.

[164] A. K. Jain, R. P. W. Duin, and J. Mao. Statistical pattern recognition: a review. *IEEE Transactions on Pattern Analysis and Machine Intelligence*, 22(1):4–37, 2000.

[165] A. K. Jain and B. Chandrasekaran. Dimensionality and sample size considerations. In P. R. Krishnaiah and L. N. Kanal, editors, *Pattern Recognition in Practice*, pages 835–855. 1982.

[166] P. Comon. Independent component analysis, a new concept? *Signal Processing*, 36(3):287–314, 1994.

[167] J. F. Cardoso. Blind signal separation: statistical principles. In *Proceedings of the IEEE*, volume 86, pages 2009–2025, 1998.

[168] K. Fukunaga. *Introduction to Statistical Pattern Recognition*. Academic Press Professional, Inc., San Diego, CA, 2nd edition, 1990.

[169] B. Schölkopf, A. Smola, and K.-R. Müller. Nonlinear component analysis as a kernel eigenvalue problem. *Neural Computing*, 10(5):1299–1319, 1998.

[170] I. Borg and P. J. F. Groenen. *Modern Multidimensional Scaling: Theory and Applications*. Springer, 2005.

[171] P. Pudil, J. Novovicova, and J. Kittler. Floating search methods in feature selection. *Pattern Recognition Letters*, 15(11):1119–1125, 1994.

[172] C. M. Bishop. *Neural Networks for Pattern Recognition*. Oxford University Press, New York, NY, USA, 1995.

[173] M. A. Hall. *Correlation-based feature selection for machine learning*. PhD thesis, The University of Waikato, 1999.

[174] H. Peng, F. Long, and C. Ding. Feature selection based on mutual information: criteria of max-dependency, max-relevance, and min-redundancy. *IEEE Transactions on Pattern Analysis and Machine Intelligence*, 27:1226–1238, 2005.

[175] B. Auffarth, M. López, and J. Cerquides. Comparison of redundancy and relevance measures for feature selection in tissue classification of CT images. In *Proceedings of the 10th Industrial Conference on Advances in Data Mining: Applications and Theoretical Aspects*, pages 248–262, 2010.

[176] R. Brunelli. *Template Matching Techniques in Computer Vision: Theory and Practice*. Wiley, 2009.

[177] T. Cover and P. Hart. Nearest neighbor pattern classification. *IEEE Transactions on Information Theory*, 13(1):21–27, 1967.

[178] P. A. Devijver and J. Kittler. *Pattern Recognition: A Statistical Approach*. Prentice Hall, London, 1982.

[179] L. Devroye, L. Gyorfi, and G. Lugosi. *A Probabilistic Theory of Pattern Recognition*. Springer, 1996.

[180] G. J. McLachlan. *Discriminant Analysis and Statistical Pattern Recognition*. Wiley Interscience, 2004.

[181] S. Raudys. Evolution and generalization of a single neuron: single-layer perceptron as seven statistical classifiers. *Neural Networks*, 11(2):283–296, 1998.

[182] L. Breiman, J. H. Friedman, R. A. Olshen, and C. J. Stone. *Classification and Regression Trees*. Wadsworth, 1984.

[183] Y. Freund and R. E. Schapire. Experiments with a new boosting algorithm. In *Proceedings of International Conference on Machine Learning*, pages 148–156, 1996.

[184] P. A. Chou. Optimal partitioning for classification and regression trees. *IEEE Transactions on Pattern Analysis and Machine Intelligence*, 13(4):340–354, 1991.

[185] C. J. C. Burges. A tutorial on support vector machines for pattern recognition. *Data Mining and Knowledge Discovery*, 2(2):121–167, 1998.

[186] J. Shawe-Taylor and N. Cristianini. *Kernel Methods for Pattern Analysis*. Cambridge University Press, 2004.

[187] L. I. Kuncheva. *Combining Pattern Classifiers: Methods and Algorithms*. Wiley-Interscience, 2004.

[188] J. A. Hartigan. *Clustering Algorithms*. John Wiley & Sons, Inc., 1975.

[189] Y. Cheng. Mean shift, mode seeking, and clustering. *IEEE Transactions on Pattern Analysis and Machine Intelligence*, 17(8):790–799, 1995.

[190] D. H. Wolpert. The lack of a priori distinctions between learning algorithms. *Neural Computing*, 8(7):1341–1390, 1996.

[191] T. G. Dietterich. Ensemble methods in machine learning. *1st Int. Work. on Multiple Classifier Systems (MCS 2000)*, *LNCS 1857*, Springer, Cagliary, pages 1–15, 2000.

[192] J. Gama and P. Brazdil. Cascade generalization. *Machine Learning*, 41(3):315–343, 2000.

[193] C. N. Silla and A. A. Freitas. Aarl survey of hierarchical classification across different application domains. *Data Mining and Knowledge Discovery*, 22(1–2):31–72, 2010.

[194] R. E. Schapire. The strength of weak learnability. *Machine Learning*, 5(2):197–227, 1990.

[195] L. Breiman. Random forests. *Machine Learning*, 45(1):5–32, 2001.

[196] R. Rulaningtyas, A. B. Suksmono, and T. L. R. Mengko. Automatic classification of tuberculosis bacteria using neural network. In *Proceedings of International Conference on Electrical Engineering and Informatics*, pages 1–4, 2011.

[197] M. G. Forero, F. Sroubek, and G. Cristóbal. Identification of tuberculosis bacteria based on shape and color. *Real-Time Imaging*, 10(4):251–262, 2004.

[198] S. Doyle, M. D. Feldman, J. Tomaszewski, and A. Madabhushi. A boosted Bayesian multiresolution classifier for prostate cancer detection from digitized needle biopsies. *IEEE Transactions on Biomedical Engineering*, 59(5):1205–1218, 2012.

[199] N. J. Fesharaki and H. Pourghassem. Medical X-ray images classification based on shape features and Bayesian rule. In *Proceedings of the 2012 Fourth International Conference on Computational Intelligence and Communication Networks*, pages 369–373, 2012.

[200] B. C. Ko, S.-H. Kim, and J.-Y. Nam. X-ray image classification using random forests with local wavelet-based CS-local binary patterns. *Journal of Digital Imaging*, 24(6):1141–1151, 2011.

[201] M. R. Zare, M. Awedh, A. Mueen, and W. C. Seng. Merging scheme-based classification of medical X-ray images. In *Proceedings of the 2011 Third International Conference on Computational Intelligence, Modelling and Simulation*, pages 253–258, 2011.

[202] N. R. Mudigonda, R. M. Rangayyan, and J. E. L. Desautels. Gradient and texture analysis for the classification of mammography masses. *IEEE Transactions on Medical Imaging*, 19(10):1032–1043, 2000.

[203] L. Zheng and A. K. Chan. An artificial intelligent algorithm for tumor detection in screening mammogram. *IEEE Transactions on Medical Imaging*, 20(7):559–567, 2001.

[204] D. Cascio, F. Fauci, R. Magro, G. Raso, R. Bellotti, F. De Carlo, S. Tangaro, G. De Nunzio, M. Quarta, G. Forni, A. Lauria, M. E. Fantacci, A. Retico, G. L. Masala, P. Oliva, S. Bagnasco, S. C. Cheran, and E. L. Torres. Mammogram segmentation by contour searching and mass lesions classification with neural network. *IEEE Transactions on Medical Imaging*, 53(5):2827–2833, 2006.

[205] M. Sameti, R. K. Ward, J. Morgan-Parkes, and B. Palcic. Image feature extraction in the last screening mammograms prior to detection of breast cancer. *IEEE Journal of Selected Topics in Signal Processing*, 3(1):46–52, 2009.

[206] L. Wei, Y. Yang, R. M. Nishikawa, and Y. Jiang. A study on several machine-learning methods for classification of malignant and benign clustered microcalcifications. *IEEE Transactions on Medical Imaging*, 24(3):371–380, 2005.

[207] A. Mayer and H. Greenspan. An adaptive mean-shift framework for MRI brain segmentation. *IEEE Transactions on Medical Imaging*, 28:1238–1250, 2009.

[208] Z. Tu and X. Bai. Auto-context and its application to high-level vision tasks and 3D brain image segmentation. *IEEE Transactions on Pattern Analysis and Machine Intelligence*, 32(10):1744–1757, 2010.

[209] C. Elliott, D. L. Arnold, D. L. Collins, and T. Arbel. Temporally consistent probabilistic detection of new multiple sclerosis lesions in brain MRI. *IEEE Transactions on Medical Imaging*, 32(8):1490–1503, 2013.

[210] V. Zagorodnov and A. Ciptadi. Component analysis approach to estimation of tissue intensity distributions of 3D images. *IEEE Transactions on Medical Imaging*, 30(3):838–848, 2011.

[211] J. Levman, T. Leung, P. Causer, D. B. Plewes, and A. L. Martel. Classification of dynamic contrast-enhanced magnetic resonance breast lesions by support vector machines. *IEEE Transactions on Medical Imaging*, 27(5):688–696, 2008.

[212] J. Yao, J. Chen, and C. Chow. Breast tumor analysis in dynamic contrast enhanced MRI using texture features and wavelet transform. *Journal of Selected Topics in Signal Processing*, 3(1):94–100, 2009.

[213] J. Detsky, G. Paul, A. Dick, and G. A. Wright. Reproducible classification of infarct heterogeneity using fuzzy clustering on multicontrast delayed enhancement magnetic resonance images. *IEEE Transactions on Medical Imaging*, 28(10):1606–1614, 2009.

[214] T. Tan, B. Platel, R. Mus, L. Tabar, R. M. Mann, and N. Karssemeijer. Computer-aided detection of cancer in automated 3-D breast ultrasound. *IEEE Transactions on Medical Imaging*, 32(9):1698–1706, 2013.

[215] H. D. Cheng, J. Shan, W. Ju, Y. Guo, and L. Zhang. Automated breast cancer detection and classification using ultrasound images: a survey. *Pattern Recognition*, 43(1):299–317, 2010.

[216] M. Moradi, P. Mousavi, A. Boag, E. Sauerbrei, R. Siemens, and P. Abolmaesumi. Augmenting detection of prostate cancer in transrectal ultrasound images using SVM and RF time series. *IEEE Transactions on Biomedical Engineering*, 56(9):2214–2224, 2009.

[217] S. Maggio, A. Palladini, L. De Marchi, M. Alessandrini, N. Speciale, and G. Masetti. Predictive deconvolution and hybrid feature selection for computer-aided detection of prostate cancer. *IEEE Transactions on Medical Imaging*, 29(2):455–464, 2010.

[218] R. Szeliski. *Computer Vision: Algorithms and Applications*. Springer, 2010.

[219] R. Davis and D. B. Lenat. *Knowledge-Based Systems in Artificial Intelligence*. Mcgraw-Hill, 1982.

[220] M. D. Levine and W. Hong. A knowledge-based approach to computer vision systems. In *Proceedings on Graphics Interface/Vision Interface*, pages 260–265, 1986.

[221] Knowledge-based systems. http://en.wikipedia.org/wiki/Knowledge-based_systems.

[222] P. Jackson and D. B. Lenat. *Introduction To Expert Systems*. Addison Wesley, 3rd edition, 1998.

[223] A. Aamodt and E. Plaza. Case-based reasoning: foundational issues, methodological variations, and system approaches. *Artificial Intelligence Communications*, 7(1):39–52, 1994.

[224] H. Shrobe, R. Davis, and P. Szolovits. What is a knowledge representation. *Association for the Advancement of Artificial Intelligence*, 14(1):17–33, 1993.

[225] D. E. Rumelhart and A. Ortony. The representation of knowledge in memory. In *Schooling and the Acquisition of Knowledge*, pages 99–135, 1977.

[226] A. Hart. *Knowledge Acquisition for Expert Systems*. McGraw-Hill, 1986.

[227] S. Perera and A. Sheth. Data driven knowledge acquisition method for domain knowledge enrichment in the healthcare. In *Proceedings of IEEE International Conference on Bioinformatics and Biomedicine*, pages 1–8, 2012.

[228] P. Domingos. Toward knowledge-rich data mining. *Data Mining and Knowledge Discovery*, 15(1):21–28, 2007.

[229] L. Getoor and B. Taskar. *Introduction to Statistical Relational Learning*. MIT Press, 2007.

[230] A. Hanson and E. Riseman. Visions: a computer system for interpreting scenes. In *Computer Vision Systems*, pages 303–333, Academic Press, New York, 1978.

[231] B. A. Draper, R. T. Collins, J. Brolio, A. R. Hanson, and E. M. Riseman. The schema system. *International Journal of Computer Vision*, 2(3):209–250, 1989.

[232] T. Matsuyama. Knowledge-based aerialimage understanding systems and expert systems for image processing. *IEEE Transactions on Geoscience and Remote Sensing*, 25(3):305–316, 1987.

[233] D. Crevier and R. Lepage. Knowledge-based image understanding systems: a survey. *Computer Vision and Image Understanding*, 67(2):161–195, 1997.

[234] S. R. Fiorini. A review on knowledge-based computer vision. 2010.

[235] B. A. Draper, A. R. Hanson, and E. M. Riseman. Knowledge-directed vision: control, learning and integration. *Proceedings of the IEEE*, 84:1625–1637, 1996.

[236] N. Lavrac, E. Keravnou, and B. Zupan. Intelligent data analysis in medicine. *Encyclopedia of Computer Science and Technology*, 42:113–157, 2000.

[237] X. Huang and J. R. Jensen. A machine-learning approach to automated knowledge-base building for remote sensing image analysis with GIS data. *Photogrammetric Engineering and Remote Sensing*, 63(10):1185–1194, 1997.

[238] B. A. Draper, K. Baek, M. S. Bartlett, and J. R. Beveridge. Recognizing faces with PCA and ICA. *Computer Vision and Image Understanding*, 91(1-2):115–137, 2003.

[239] M. E. Leventon, W. E. L. Grimson, and O. Faugeras. Statistical shape influence in geodesic active contours. In *Proceedings of IEEE International Conference on Computer Vision and Pattern Recognition*, pages 316–323, 2000.

[240] K. Etemad and R. Chellappa. Discriminant analysis for recognition of human face images. *Journal of Optical Society of America A*, 14:1724–1733, 1997.

[241] E. A. Vokurka, A. Herwadkar, N. A. Thacker, R.T. Ramsden, and A. Jackson. Using bayesian tissue classification to improve the accuracy of vestibular schwannoma volume and growth measurement. *AJNR American Journal of Neuroradiology*, 23(3):459–467, 2002.

[242] A. Onisko, P. J. F. Lucas, and M. J. Druzdzel. Comparison of rule-based and bayesian network approaches in medical diagnostic systems. In *Proceedings of the Eighth Conference on AI in Medicine in Europe: Artificial Intelligence Medicine, AIME'01*, pages 283–292, 2001.

[243] I. Cohen, N. Sebe, F. G. Gozman, and M. C. Cirelo. Learning bayesian network classifiers for facial expression recognition both labeled and unlabeled data. In *Proceedings of IEEE International Conference on Computer Vision and Pattern Recognition*, pages 595–601, 2003.

[244] P. Zhong. Learning conditional random fields for classification of hyperspectral images. *IEEE Transactions on Image Processing*, 19(7):1890–1907, 2010.

[245] N. Plath, M. Toussaint, and S. Nakajima. Multi-class image segmentation using conditional random fields and global classification. In *Proceedings of the Twenty Sixth International Conference on Machine Learning*, pages 817–824, 2009.

[246] F. Monay and D. Gatica-Perez. On image auto-annotation with latent space models. In *Proceedings of the Eleventh ACM International Conference on Multimedia*, pages 275–278, 2003.

[247] G. E. Hinton, S. Osindero, and Y. W. Teh. A fast learning algorithm for deep belief nets. *Neural Computation*, 18(7):1527–1554, 2006.

[248] F. Niu, C. Zhang, C. Ré, and J. W. Shavlik. Elementary: large-scale knowledge-base construction via machine learning and statistical inference. *International Journal on Semantic Web and Information Systems*, 8(3):42–73, 2012.

[249] G. Rizzo, P. Scifo, M. C. Gilardi, V. Bettinardi, F. Grassi, S. Cerutti, and F. Fazio. Matching a computerized brain atlas to multimodal medical images. *NeuroImage*, 6(1):59–69, 1997.

[250] M. C. Clark, L. O. Hall, D. B. Goldgof, R. Velthuizen, F. R. Murtagh, and M. S. Silbiger. Automatic tumor segmentation using knowledge-based techniques. *IEEE Transactions on Medical Imaging*, 17(2):187–201, 1998.

[251] T. McInerney and D. Terzopoulos. Deformable models in medical image analysis: a survey. *Medical Image Analysis*, 1(2):91–108, 1996.

[252] I. El-Naqa, Y. Yang, M. N. Wernick, N. P. Galatsanos, and R. M. Nishikawa. A support vector machine approach for detection of microcalcifications. *IEEE Transactions on Medical Imaging*, 21(2):1552–1563, 2002.

[253] H. J. Lowe, I. Antipov, W. Hersh, and C. A. Smith. Towards knowledge-based retrieval of medical images. The role of semantic indexing, image content representation and knowledge-based retrieval. In *Proceedings of the AMIA Symposium*, pages 882–886, 1998.

[254] NIH. Unified medical language system. http://www.nlm.nih.gov/research/umls/.

[255] W. Wei and P. M. Barnaghi. Semantic support for medical image search and retrieval. In *Proceedings of the Fifth IASTED International Conference: Biomedical Engineering*.

[256] B. Hu, S. Dasmahapatra, P. Lewis, and N. Shadbolt. Ontology-based medical image annotation with description logics. In *Proceedings of Fifteenth IEEE International Conference on Tools with Artificial Intelligence*.

[257] L. Temal, M. Dojat, G. Kassel, and B. Gibaud. Towards an ontology for sharing medical images and regions of interest in neuroimaging. *Medical Image Analysis*, 41(5):766–778, 2008.